UCSF
UC San Francisco Electronic Theses and Dissertations

Title
Nerve growth factor

Permalink
https://escholarship.org/uc/item/5132938j

Author
Chua-Couzens, Jane,

Publication Date
1995

Peer reviewed|Thesis/dissertation

eScholarship.org Powered by the California Digital Library
University of California

NERVE GROWTH FACTOR: EFFECTS ON SURVIVAL OF DEVELOPING SEPTAL CHOLINERGIC NEURONS

by

JANE CHUA-COUZENS

THESIS

Submitted in partial satisfaction of the requirements for the degree of

MASTER OF SCIENCE

in

ORAL BIOLOGY

in the

GRADUATE DIVISION

of the

UNIVERSITY OF CALIFORNIA

San Francisco

Ap

Da

De

DEDICATION

To Amah, Pa and Ma
whose example of faith, courage, perseverance and hardwork
made this work possible

To Mom
for her friendship and encouragement

To David
for his wonderful gift of love

UCSF LIBRARY

ACKNOWLEDGMENTS

The completion of this thesis entailed invaluable contributions from a number of colleagues. I would like to express my sincere gratitude to:

My mentor, Dr. William Mobley, who gave me the opportunity to join his laboratory and to learn with him. His careful scientific analyses and interpretations have left an imprint in my mind that is and will be invaluable in time to come, and his approach of serious science combined with a human touch will always be deeply appreciated.

Drs. Jon Levine, Peter Sargent and Robert Stern, for agreeing to serve in my thesis comittee, and whose interest and enthusiasm in this work had been a great encouragement.

Dr. David Holtzman, for the many discussions we had at the start of this project, for teaching me the surgical techniques used in this work, and for his comments and suggestions in the manuscript.

Dr. Ron Siegel, who unselfishly shared his expertice and assistance in the fabrication of the polymer implants used in this study.

Dr. Peter Mouton, who came all the way from Johns Hopkins University to give a seminar and get me started on stereology.

Dr. Yiwen Li and Ms. Janice Valletta, who have been invaluable in providing day-to day answers to technical questions in immunohistochemistry and bioassays.

Mr. Michael Callaghan, for the many milligrams of NGF preparations used in the injections, implants and osmotic pumps.

Mr. Joshua Kilbridge, who patiently coded each histology slides in preparation for stereology.

UCSF LIBRARY

Dr. Deborah Hall, for reading the manuscript and for encouragement in the final preparation of this work.

Finally, to my husband David, who worked so hard in making me cut my long, winded sentences, for copy editing the manuscript and most of all, for being there every single day.

UCSF LIBRARY

NERVE GROWTH FACTOR; EFFECTS ON THE SURVIVAL OF DEVELOPING SEPTAL CHOLINERGIC NEURONS

Jane Chua-Couzens

Abstract

Nerve growth factor (NGF) is a neurotrophic factor for basal forebrain cholinergic neurons (BFCNs). It has been shown that NGF supports the morphological and biochemical differentiation of these neurons during development. Also, NGF acts to enhance the survival and maintenance of axotomized adult cholinergic neurons. However, it is uncertain whether these neurons are subject to death during development and whether or not they compete for NGF for their survival during this period. We reasoned that if the survival of these cells is regulated through competition for limiting quantities of target-derived NGF, then administering NGF to achieve supraphysiologic levels should result in survival of all such neurons. In this study, we used implants to administer exogenous NGF to postnatal rats during the first month of life. Carrier protein containing implants serve as controls. NGF infusion via cannula was given to both groups from PD29-PD35 to ensure detection of cholinergic neurons. The brains of subjects were sectioned and immunostained for choline acetyl transferase (ChAT), a marker for cholinergic neurons. The number of ChAT-positive neurons in the medial septal nucleus was counted using unbiased stereological methods. Results showed that marked increases in NGF failed to increase the number of septal BFCNs. These data suggest that either BFCNs are not dependent on NGF for their survival in the early postnatal period or that NGF levels normally present at this time are sufficient to ensure their survival.

UCSF LIBRARY

TABLE OF CONTENTS

UCSF LIBRARY

LIST OF FIGURES

UCSF LIBRARY

LIST OF TABLES

ABBREVIATIONS

AChE = acetylcholinesterase

BDNF = brain-derived neurotrophic factor

BFCNs = basal forbrain cholinergic neurons

BV = biological variance

CE = coefficient of error

ChAT = choline acetyl transferase

CNS = central nervous system

CNTF = ciliary neurotrophic factor

CSF = cerbrospinal fluid

CV = coefficient of variance

DRG = dorsal root ganglia

ED = embryonic day

ELISA = enzyme-linked immunosorption assay

EVAc = poly-ethylene-covinyl acetate

FGF = fibroblast growth factor

FCS = fetal calf sreum

GAM = polyclonal goat anti-mouse NGF

GIG = preimmune goat serum

ICV = injection into the lateral cerebral ventricle

1G3 = monoclonal anti-rat NGF

mRNA =message RNA

MSN = medial septal nucleus

NGF = Nerve growth factor

NGF_{180} = NGF implants made with <180 μm NGF/RSA powder

NGF_{250} = NGF implants made with <250 μm NGF/RSA powder

NGF_{90} = NGF implants made with <90 μm NGF/RSA powder

NRS = normal rabbit serum

NT-3 = neurotrophic factor-3

N_V = numerical density

$p75^{NGFR}$ = low-affinity NGF receptor

PBS = phosphate buffered saline

PBST = phosphate buffered saline + 0.1% tween 20

PD = postnatal day

PNS = peripheral nervous system

RSA = rat serum albumin

RSA_{180} = RSA implants made with <180 μm RSA powder

RSA_{250} = RSA implants made with <250 μm RSA powder

RSA_{90} = RSA implants made with <90 μm RSA powder

SA-HRP = strepavidin horeseradish peroxidase

SCG = superior cervical ganglion

SD = standard deviation

SEM = standard error of the mean

TBS = tris buffered saline

TBST = tris buffered saline + 0.3% triton x 100

TG = trigeminal ganglion

trk A = high-affinity NGF receptor

TUNEL = terminal dUTP nick-end labeling

UNT = untreated

VEH = vehicle treated

$Vol_{(MSN)}$ = volume of the mesial septal nucleus

Chapter 1

INTRODUCTION

1.1 Nerve growth factor

Nerve growth factor (NGF) is a polypeptide neurotrophic factor and a member of the neurotrophin gene family. Its discovery by Levi-Montalcini and her colleagues some 40 years ago established NGF as the first neurotrophic factor, and it has been extensively studied (Levi-Montalcini and Hamburger, 1951, Levi-Montalcini, 1987, Longo, et al., 1993). NGF-responsive neurons are found in both the peripheral nervous system (PNS) and central nervous system (CNS) (Levi-Montalcini and Angeletti, 1968, Thoenen and Barde, 1980, Heumann, et al., 1984b, Korsching, et al., 1985, Holtzman, et al., 1992, Holtzman, et al., 1994). NGF acts via binding to the cell surface receptors $p75^{NGFR}$ and trk A. Binding to the latter accounts for many, if not all, NGF actions on neurons (Loeb, et al., 1991, Chao, 1992, Meakin, et al., 1992a). NGF robustly enhances neuronal differentiation in both the PNS and the CNS. However, increased survival of developing PNS neurons is perhaps the most dramatic response to NGF. This action is presumed to reflect a role for target-derived NGF in regulating the death of these neurons during normal development (Longo, et al., 1993). Several observations support this contention. First, there are convincing demonstrations for the importance of NGF in preventing death of responsive PNS neurons (Levi-Montalcini and Cohen, 1956, Hendry and Campbell, 1976, Hamburger, et al., 1981, Martin and Johnson, 1991, Server and Mobley, 1991). For example, while NGF increases the viability of cultured sympathetic neurons and causes them to mature, its withdrawal leads to degeneration of neurites and cell death (Martin and Johnson, 1991). Equally impressive results have been achieved in vivo. Levi-Montalcini and colleagues were the first to administer NGF to

chick embryos. Following treatment for 3-5 days, there was overgrowth of sensory and sympathetic ganglia and excessive production of neurites (Levi-Montalcini and Cohen, 1956). Conversely, administration of NGF antibodies to neonatal rats resulted in near complete destruction of sympathetic neurons (Levi-Montalcini and Booker, 1960). Second, there are conclusive data for production of NGF in the targets of sensory and sympathetic neurons (Heumann, et al., 1984a, Shelton and Reichardt, 1986, Davies, et al., 1987). Finally, experimental manipulation of the target fields of NGF-responsive neurons has provided evidence that target-derived NGF is important for neuronal viability. Removal of the submandibular gland of neonatal mice results in the failure of normal development of neurons in the superior cervical ganglion (SCG), which innervate this gland. Conversely, if the gland was replaced by a preparation in which NGF was linked to cellulose, SCG neurons developed normally (Hendry and Iversen, 1973). These data combine to support strongly the hypothesis that target-derived NGF regulates the survival of responsive PNS neurons during development.

In the past decade, research on programmed cell death, (also called physiological or naturally occuring cell death) has focused increased attention on NGF actions in inhibiting death of developing neurons, and recent studies are providing novel insights into how PNS neurons die when deprived of NGF (Martin and Johnson, 1991, Estus, et al., 1994, Franklin, et al., 1995). Given its PNS actions, and the dramatic effects of exogenous NGF on CNS neuron differentiation, it has been suggested that NGF also regulates survival of developing CNS neurons. Indeed, exogenous NGF has been shown to prevent death of axotomized basal forebrain cholinergic neurons (BFCNs) (Hefti, 1986). However, the physiologic role of endogenous NGF on developing CNS neurons is only now being explored. Whether or not NGF is important for viability of these neurons during development is yet to be established. Understanding whether this is the case, and if so, how death of CNS neurons is prevented by NGF would provide an important perspective on CNS development. Also, it is reasonable to suggest that the mechanism

of death in developing neurons might apply to neurons that die during aging and in the setting of neurodegenerative diseases. Thus, understanding NGF actions relative to the physiological death of CNS neurons might help to unravel the pathogenesis of devastating neurodegenerative diseases.

In the experiments described herein, we have focused on NGF actions on developing BFCNs. These neurons degenerate in Alzheimer's disease and their loss appears to contribute to cognitive problems and memory impairment (Koh, et al., 1989b, Fischer, et al., 1991). The studies reported herein tested the idea that NGF normally regulates the viability of these cells during development.

1.2 Naturally occuring cell death

Cell death occurs naturally in a large number of tissues during vertebrate development. It appears to play an important role in establishing the mature form and function of the organism (Glucksmann, 1951, Saunders, 1966). In the PNS, neurons are normally overproduced and are then through programmed cell death pared down so that the size of the neuronal centers (i.e. sensory and sympathetic ganglia and motor neuron nuclei) are matched to the size of their target tissues (Cowan, 1984, Williams and Herrup, 1988, Oppenheim, 1991). In the vertebrate CNS, cell death balances mitosis and differentiation to determine the ontogeny of the brain (Cunningham, et al., 1982, Oppenheim, 1989, Oppenheim, et al., 1990, Oppenheim, 1991, Catsicas, et al., 1992). Studies on naturally occuring cell death in the developing nervous system have demonstrated that about 50% of neurons die during normal development (Davies and Lumsden, 1984, Davies, et al., 1987). As a result of observations from a large body of work on neuronal death and from studies on the actions of NGF and other trophic factors, the neurotrophic factor hypothesis was advanced. This states that death results from limited availability of trophic factors supplied by the target (Barde, 1989, Server and Mobley, 1991, Longo, et al., 1993). Cells that have a sufficient supply of trophic

UCSF LIBRARY

factors live, and those that do not die. Recent studies have suggested that in order to die, cells must activate an autonomous, genetically encoded death program (Martin, et al., 1988, Oppenheim, et al., 1990, Scott and Davies, 1990, Garcia, et al., 1992, Hengartner, et al., 1992, Allsopp, et al., 1993). It has been argued that this program is negatively regulated by trophic factors and that in the absence of the proper trophic factor(s), the death program would be activated. Thus, sufficient NGF within the immediate environment of the axon of responsive neurons would block the death program and lead to survival; conversely, removal of NGF would result in lifting the block to the death program, thus allowing the neuron to seek its own demise (Martin and Johnson, 1991). The hypothesis predicts that by removing NGF during development, when natural cell death is occurring, the death process would be exaggerated. On the other hand, if excess NGF was given at this critical time, the death process should be aborted and neurons rescued from developmental death. Work in the PNS provides considerable evidence to support this idea. Neutralization of endogenous NGF via NGF antibodies in prenatal rats resulted in the near total loss of sensory neurons (Johnson and Gorin, 1980). Postnatal administration of NGF antibodies resulted in marked loss of sympathetic neurons but had no effect on sensory neurons (Levi-Montalcini and Booker, 1960). Thus, the timing of antibody administration was critical in determining which cells would die. Significantly, sensory neurons undergo cell death prenatally while most sympathetic neurons die during early postnatal life (Levi-Montalcini and Booker, 1960, Johnson and Gorin, 1980). Complementing these findings, administration of exogenous NGF has been shown to prevent death of sensory and sympathetic neurons (Hendry, 1975, Johnson and Gorin, 1980, Thoenen and Barde, 1980, Cunningham, et al., 1982, Heumann, et al., 1984b, Korsching and Thoenen, 1985, Eichler and Rich, 1989). These data give strong support to the hypothesis that through limited availability, NGF is responsible for regulating the death of sensory and sympathetic neurons. Additional support has come from recent studies

using gene knockouts for NGF and trk A (Crowley, et al., 1994, Smeyne, et al., 1994). NGF null mutant mice exhibited severe cell loss in sympathetic ganglia and selective cell loss in sensory ganglia (Crowley, et al., 1994). Mutant mice carrying a disrupted trk A gene displayed massive loss of trigeminal neurons. The dorsal root ganglia (DRG) also exhibited extensive loss (70-90%) of small neurons, and there were very few sympathetic neurons present in the SCG (Smeyne, et al., 1994). Thus, it appears that target-derived NGF has a critical role in regulating the developmental death of PNS neurons.

1.3 NGF actions in the CNS

NGF actions in the CNS have been best characterized in cholinergic neurons of the striatum and in BFCNs. The latter includes the septo-hippocampal cholinergic system, which comprises cholinergic neurons in the medial septal nucleus (MSN) and their axons, which project to the hippocampus (Butcher and Woolf, 1983, McGeer, et al., 1983). MSN cholinergic neurons project their axons mainly to the ipsilateral hippocampus (Sofroniew, et al., 1990). NGF has robust actions on these cells. Several lines of evidence have suggested a physiologic role for NGF: 1) the hippocampus, which is the main target of septal cholinergic neurons, contains the highest concentration of NGF mRNA and NGF protein in the CNS (Shelton and Reichardt, 1986); 2) the genes for the NGF receptors, trk A and $p75^{NGFR}$, are expressed in BFCNs (Cavicchioli, et al., 1989, Higgins, et al., 1989, Holtzman, et al., 1992, Holtzman, et al., 1994, Li, et al., 1994); 3) NGF binds to BFCNs (Richardson and Riopelle, 1984, Altar and Bakhit, 1991) and is retrogradely transported from the hippocampus to the medial septum (Schwab, et al., 1979, Seiler and Schwab, 1984); 4) NGF also acts in BFCNs to regulate the activity of genes important in BFCN development (Gnahn, et al., 1983, Mobley, et al., 1985, Mobley, et al., 1986, Johnston, et al., 1987, Mobley, et al., 1988, Mobley, et al., 1989, Holtzman, et al., 1992, Li, et al., 1994, Holtzman, et al., 1995); and 5) neonatal

rats treated with specific NGF antibodies showed decreased choline acetyl transferase (ChAT) and trk A gene expression in the MSN, and suppression of the the normal developmental increase in BFCN cell size (Li, et al., 1994). NGF actions extend to impaired and aged neurons. Exogenous NGF prevented atrophy and death of BFCNs following axotomy (Hefti, 1986, Williams, et al., 1986, Kromer, 1987, Hoffman, et al., 1990, Koliatsos, et al., 1991) and enhanced spatial memory in aged-impaired rats (Fischer, et al., 1991, Markowski, et al., 1994). Taken together, these data point to robust actions of NGF on BFCNs and to the probability that NGF actions are physiologically significant.

1.4 Understanding NGF actions in the developing septo-hippocampal system

Endogenous NGF appears to have an important role in enhancing the biochemical and morphological differentiation of BFCNs. During development, the appearance of NGF in the hippocampus and the septum anticipates by several days the development of other markers of differentiation of BFCNs. NGF mRNA is detected before NGF protein, and increases in NGF are seen before increases in ChAT mRNA, trk A mRNA and $p75^{NGFR}$mRNA (Large, et al., 1986, Auburger, et al., 1987) (see Table 2). Morphological maturation, manifested by the increase in cell size of MSN cholinergic neurons, demonstrates a pattern similar to that for the neurochemical markers (Li, et al., 1994). These data, those cited for the effects of NGF antibody injections, and for the consequences of disrupting the genes for NGF and trk A indicate that NGF regulates BFCN differentiation. However, they do not address a role for NGF in regulating the survival of these cells. Indeed, no published study has established that death does occur in BFCNs during development. Nevertheless, the fact that neurons die during

development in most PNS and CNS populations makes it likely that developmental death also occurs in developing BFCNs.

NGF appears to act on BFCNs essentially as soon as their axons reach the hippocampus. The differentiation of BFCNs entails growth of axons from the MSN to the hippocampus and their subsequent elaboration and organization between embryonic day (ED) 17 and postnatal day (PD) 21 (see Table 1). NGF is present in the hippocampus at ED 17 (see Table 2). Thus, initial NGF production appears to slightly anticipate arrival of cholinergic axons and to be independent of it. The majority of septal axons arrive in the hippocampus (Table 1) at postnatal day 0 (PD 0 = day of birth). At this time (see Table 2), NGF mRNA in the hippocampus increases while the NGF protein level drops to barely detectable (Auburger, et al., 1987). The decrease in NGF protein has been interpreted as being due to the onset of retrograde transport of NGF from the hippocampus to the septum. Significantly, trk A mRNA and protein are present in BFCNs at PD 0 and these cells demonstrate responses to NGF in the very early postnatal period (Johnston, et al., 1987). Thus BFCNs appear to be NGF-responsive during essentially the entire postnatal period.

UCSF LIBRARY

1.5 Predicting the period for death in developing BFCNs

A review of relevant data for NGF-responsive PNS neurons allows us to predict when developmental death is likely to occur in BFCNs. Developmental cell death in the PNS usually occurs soon after the establishment of axonal contact with the target (Wright, et al., 1983, Davies, et al., 1987). For example, in the case of rat SCG neurons, the first sympathetic axons enter the target at ED 15 (see Figure 1.1a). By ED 18-19, all axons arrive in their target. Wright et al (1983) reported apparent onset of SCG degeneration by ED 19 or 20 with most cell death occuring between ED 19 and PD 3. The timing of cell death for SCG neurons can be compared to that of NGF gene

expression and NGF actions. At ED15, when the first axons reached their target, NGF is present in the submandibular gland and the level increases over the next few days. NGF levels in the SCG mirror those in the submandibular gland (Figure 1.1d), probably reflecting retrograde transport of NGF to SCG neuron cell bodies (Korsching and Thoenen, 1983). In vitro studies have shown NGF responsiveness of these cells by ED 14 (Coughlin and Collins, 1985). Functional NGF receptor proteins are present by ED 17 (see Figure 1.1c). Thus, cell death ensues after target contact and occurs in the presence of NGF in the target (Figure 1.1b) and functional NGF receptors on SCG neurons. In studies on the mouse trigeminal ganglion (TG) (see Figure 1.2a), Davies and colleagues showed that sensory neurons are born at ED 9.5. At ED 11, the first axons contact the epithelium of the maxillary process, and the last axons arrive just after ED 15. Sensory neuron number peaks at ED 13. Cell death, which begins at ED 13 and continues through ED 19 (birth), results in the loss of over 50% of neurons (Davies and Lumsden, 1984, Davies, et al., 1987). In the target tissues of the TG (see Figure 1.2b), NGF mRNA is first detected at ED 10.5, 12 hours before the detection of NGF protein. By ED11, when the first axons reach the epithelium of the maxillary process, NGF protein is present. NGF protein levels showed a dramatic decrease at ED 13, while NGF mRNA continued to increase and peaks at ED 15. Within the TG, NGF protein was first detected at ED12, 24 hours after the first axons reached their target (Figure 1.2d). As for sympathetic neurons, functional NGF receptors are present prior to target contact (Figure 1.2c). Thus, mouse TG neurons follow a developmental pattern similar to rat SCG neurons.

We can use the timing of developmental events in these other systems to predict the time for cell death among BFCNs. In the PNS, it is clear that: 1) target contact precedes onset of cell death; 2) cell death extends over several days, lasting beyond the time for completion of target contact; and 3) NGF production in the target commences at or about the time of target contact. Translating this to BFCNs, one would predict

UCSF LIBRARY

onset of cell death at or near PD 0 with continued cell loss over the next several days, i.e. beyond the point at which BFCN axons have entered the hippocampus. In planning our studies, uncertainty regarding the timing of the cell death period encouraged us to extend this period to the last possible time for occurrence of developmental events. Logically, this is at the end of development, which for BFCNs is approximately PD 30. Thus, we set out to deliver an excess amount of NGF to the hippocampus to encompass the entire first postnatal month.

1.6 Mode of long-term NGF delivery

Our goal was to deliver NGF so as to achieve continuous supraphysiologic levels (at least 10 times the endogenous level) in the hippocampus of neonatal rats for 28 days. In the past, successful delivery of pharmacologic doses of NGF was accomplished by direct intraventricular injection into the lateral cerebral ventricle (ICV) of the rat (Mobley, et al., 1985, Mobley, et al., 1986, Mobley, et al., 1989, Yan, et al., 1994). This method is very useful in experiments involving short-term NGF delivery. However, we found that when more than 3 or 4 of these injections are given every other day, hydrocephalus ensues. In addition, NGF delivered by ICV injections is cleared in 48 hrs. (see Section 2.2 and 2.3). Thus, to maintain relatively high NGF levels by ICV injection would entail giving injections every day.

The polymer implant system, wherein NGF could be slowly released over a prolonged period (Siegel and Langer, 1984, Siegel and Langer, 1990), appeared much better suited to our needs. Others had used this system by placing an NGF-releasing implant into the lateral ventricle of adult rats for a period of 2 weeks (Hoffman, et al., 1990). However, we envisioned the possibility that placing an implant in the intraventricular space of a neonatal rat would result in injury to the ventricular system,

Table 1 **Time course of development of the septo-hippocampal system** (summarized from Koh and Loy, 1989a, Milner, et al., 1983, Li, et al., 1995).

Age in days	**Histological observation**
ED 14	hippocampal anlage identified
ED15	MSN/diagonal band precursors identified
ED 17	end of mitosis of septal cholinergic neurons (i.e. septal BFCNs)
ED 17- ED 21	first septal BFCN axons arrive in hippocampus
PD 0	majority of septal BFCN axons have arrive in hippocampus
ED 17- PD 21	septal BFCN size increases
PD 30	septal BFCN size decreases to adult size

Table 2 **Time course for NGFmRNA, NGF protein expression, and ChAT activity during development of the septo-hippocampal system** (summarized from Auburger, et al., 1987, Large, et al., 1986, Li, et al., 1995)

		mRNA^{NGF}	**NGF**	**ChAT**	**trk A**
Hippocampus	Prenatal	no data	*ED 17*, relatively high	*ED 17*, very low	
	Post-natal	*PD 0*, detected; *PD 1-6*, gradual increase; *PD 6-9*, rapid increase; *PD 20*, peak	*PD 0-2*, relatively low; *PD 2-12*, gradual increase; *PD 12-14*, rapid increase; *PD 20*, peak; *PD 30*, adult level	*PD 0-12*, gradual increase; *PD 12-14*, rapid increase; *PD 20*, peak	*PD 4*, barely detectable; *PD 21*, markedly increased to greater than adult level
Septum	Post-natal		*PD 0-12*, gra-dual increase; *PD 12-18*, rapid increase; *PD 20*, peak	*PD 0*, barely detectable; *PD 8-20*, rapid increase; *PD 22*, peak	*PD 4*, detectable; *PD 21*, markedly increased, equal to adult level

Development of the rat superior cervical ganglia (SCG)

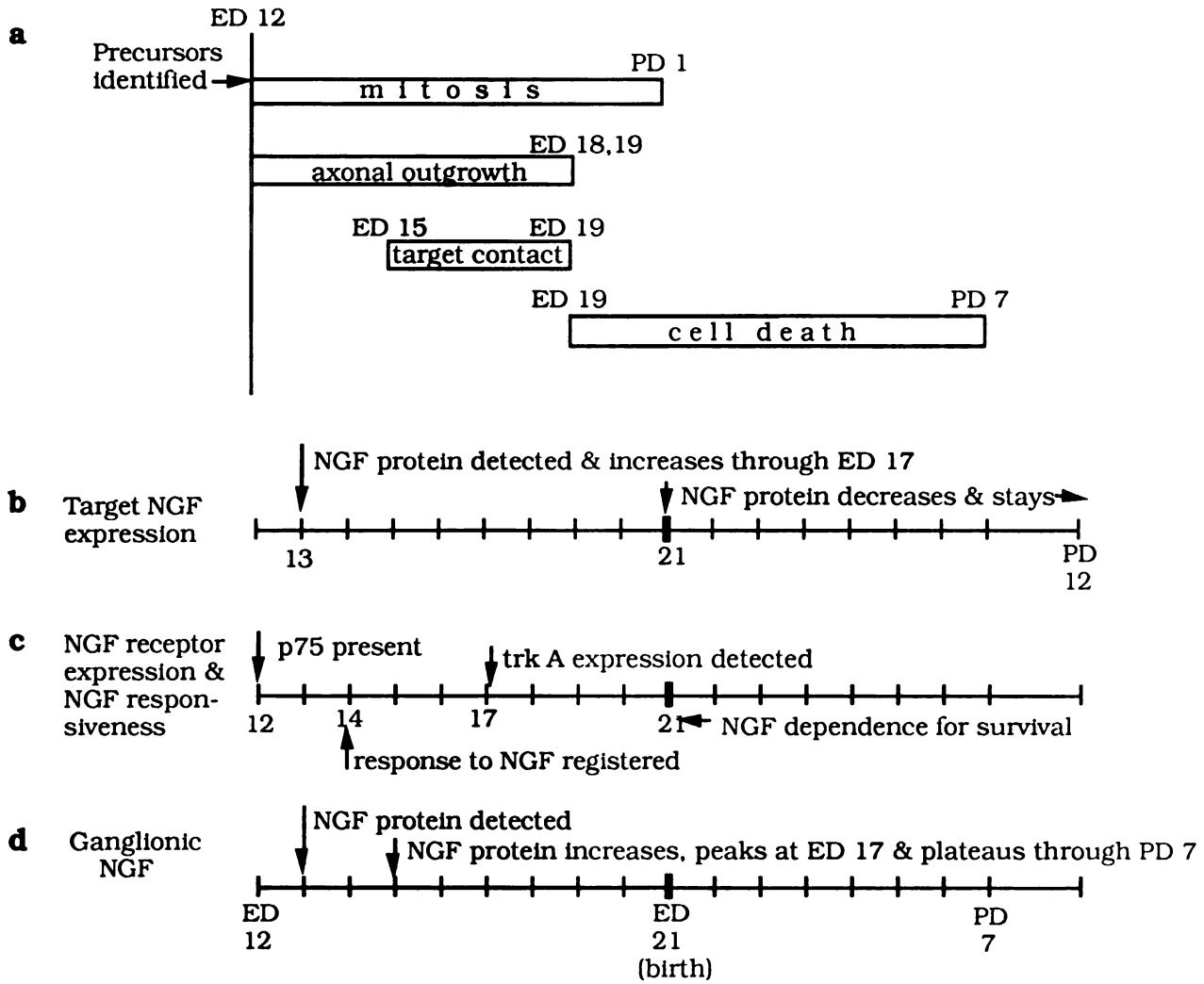

Figure 1.1 a Developmental events for sympathetic neurons

b Target NGF expression

c NGF receptor expression and NGF responsivenes

d Ganglionic NGF levels

(summarized from Longo, et al, 1993, Wright et al,1983)

ULST LIBRARY

Development of the mouse trigeminal ganglia (TG)

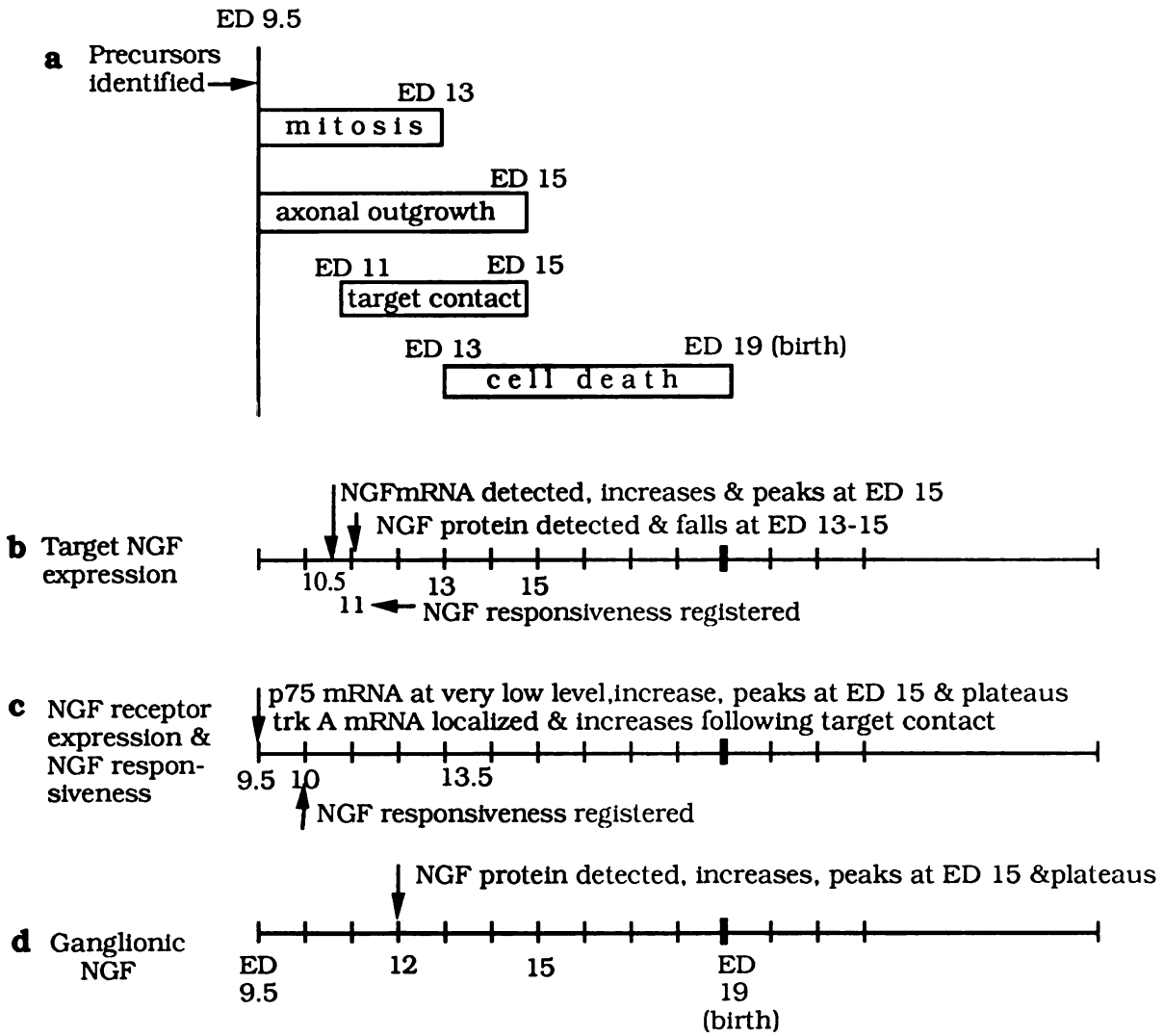

Figure 1.2 a Developmental events for sensory neurons

b Target NGF expression

c NGF receptor expression and NGF responsiveness

d Ganglionic NGF levels

(summarized from Longo et al,1993 and Davies et al, 1984)

UCSF LIBRARY

Chapter 2

SLOW RELEASE DELIVERY SYSTEM

ETHYLENE VINYL ACETATE COPOLYMER IMPLANTS

2.1 Background

The use of porous organic matrices as a vehicle for slow drug release has been explored since the 1980s (Rhine, et al., 1980, Murray, et al., 1983, Siegel and Langer, 1984, Bawa, et al., 1985). One such matrix, that has become the subject of extensive study, is based on poly-ethylene-covinyl acetate (EVAc). This polymer system is created by uniformly dispersing carefully sized particles of the drug into an organic EVAc solution, followed by the evaporation of the solvent. The final product is an inert matrix laden with pores that are occupied by the drug powder particles. These pores form interconnecting "throats" creating a continuous network of pores (see Figure 2.1 for a schematic diagram of this porous network). The release of drug from the pores is due to simple diffusion down a concentration gradient. Under physiological conditions, water or tissue fluids dissolves particles first in the pores, the high drug concentration in the pores then allows for the progressive release of the drug into the tissue, where drug concentration is low. The mechanism accounting for the slowness of drug release was studied by Siegel et al (1990). Drug in pores at the cut surface of the polymer matrix readily diffused out into the tissue space. However, to release drug contained in pores deep within the matrix, water or tissue fluids must first dissolve the material in the deeper pores. Dissolved drug then diffuses through previously vacated throats and pores to gain access to the tissue space.

Successful use of this delivery system depends mainly on the creation of a labyrinth of pores formed by the drug and its carrier. As a consequence, two factors

ULST LIBRARY

govern the formation of this intricate network: the loading volume and the particle size of the drug and its carrier. The loading volume determines: 1) the "closeness" of the pores within the matrix, i.e. the higher the loading volume, the closer the pores, and 2) the probability of forming interconnecting "throats" as a result of 1), i.e. the farther apart the pores, the lesser is the probability of forming interconnecting throats. The particle size of the drug mainly determines the tortuosity of the pore formation, but it also contributes to the "closeness " of pores within the matrix (see Figure 2.1).

In this study, the slow release system, in the form of an intracranial implant, was chosen to deliver NGF into the hippocampus for a period of 28 days.

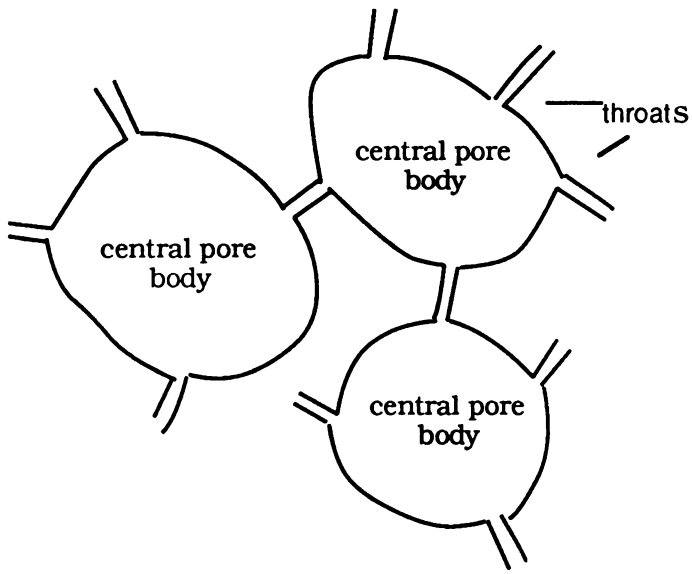

Figure 2.1 Two-dimensional schematic of pore geometry (modified from Siegel et al., 1990)

2.2 Calculating the amount of NGF to be incorporated into implants

The ultimate goal of this delivery system was to establish supraphysiologic levels of NGF—10 times higher than baseline adult levels, or about 10 ng NGF/g brain

UNSW LIBRARY

tissue—in the hippocampus and the septum. To achieve this goal, the clearance rate of NGF in the hippocampus and septum had to be determined. This value was used to ascertain the rate of NGF delivery. In turn, the rate of delivery was used to calculate the amount of NGF needed to be incorporated into each implant.

2.2a NGF clearance experiment

NGF prepared from the mouse submaxillary gland (Mobley, et al., 1986) was sterilized by passing it through .22 µm filters (Millipore™). It was then quick frozen, lyophilized overnight, and dissolved in filtered phosphate buffered saline (PBS)-acetic acid solution (4 parts PBS to 1 part of 0.05% acetic acid, pH 7.0) to a concentration of 6 µg/µl.

Five microliters of NGF (30 µg total) or vehicle (PBS–acetic acid solution alone) were injected directly into the right lateral cerebral ventricle of 7-day-old rat pups (PD7) using a 20 microliter Hamilton syringe with a 26S, beveled. The point of entry was 1.2 mm lateral to the superior sagittal sinus, 1.5 mm rostral to the lateral sinus, and the needle was inserted to a depth of 1.5 mm. At 2, 6, 12, 24, 48, 72, and 120 hours after injection, the brain was dissected and the right and left septum and hippocampus were collected. NGF levels in these tissues were then determined using a highly sensitive and specific enzyme linked immunosorption assay—ELISA (Weskamp and Otten, 1987) (see Appendix B for brain dissection and ELISA protocol). NGF levels were measured in the same tissues in untreated rat littermates at PD 7, 8, 9, and 10.

2.2b NGF clearance in the hippocampus and septum

The results of the clearance experiment are shown in Figure 2.2. Two- and six-hour data points are not shown as the value obtained from ELISA was higher than the highest NGF value in the standard curve. At 12 hours after ICV administration of NGF, the level in the hippocampus measured 311 ng NGF/g tissue. This was 0.1% of the NGF

UCSF LIBRARY

dose. At 24 hours after injection, about 75 ng NGF/g tissue, or 0.025% of the NGF dose was retained in the hippocampus. At 48 hours, the NGF level in the hippocampus had dropped to baseline values (i.e. the value present in the untreated hippocampus).

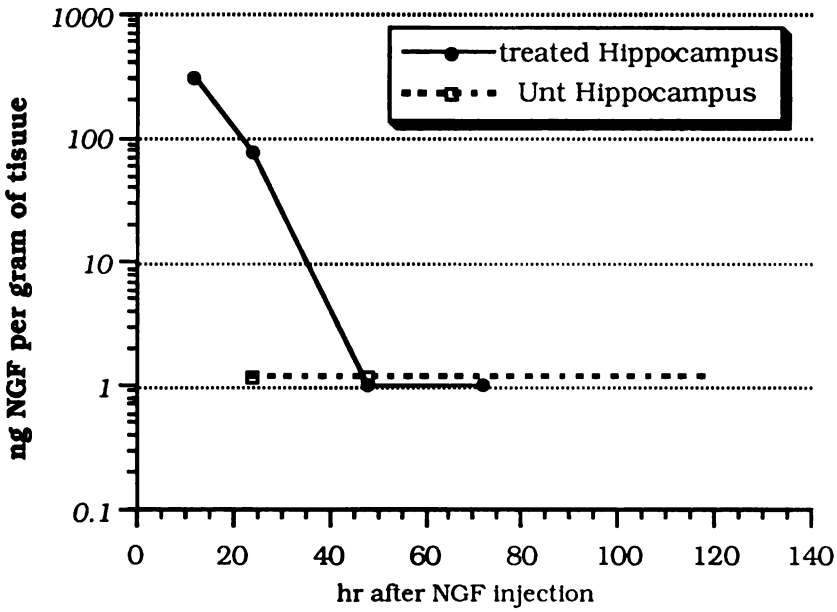

Figure 2.2 NGF clearance in the hippocampus

The same pattern for clearance was seen in the septum (Figure 2.3). The NGF levels were: 1) 6-hours after injection = 96.2 ng/g tissue, or 0.02% of NGF dose; 2) 12-hours after injection = 57 ng/g, or 0.01% of NGF dose; 3) 24-hours after injection = 15 ng/g, or 0.002% of initial dose; and 4) baseline values 48 hours after administration.

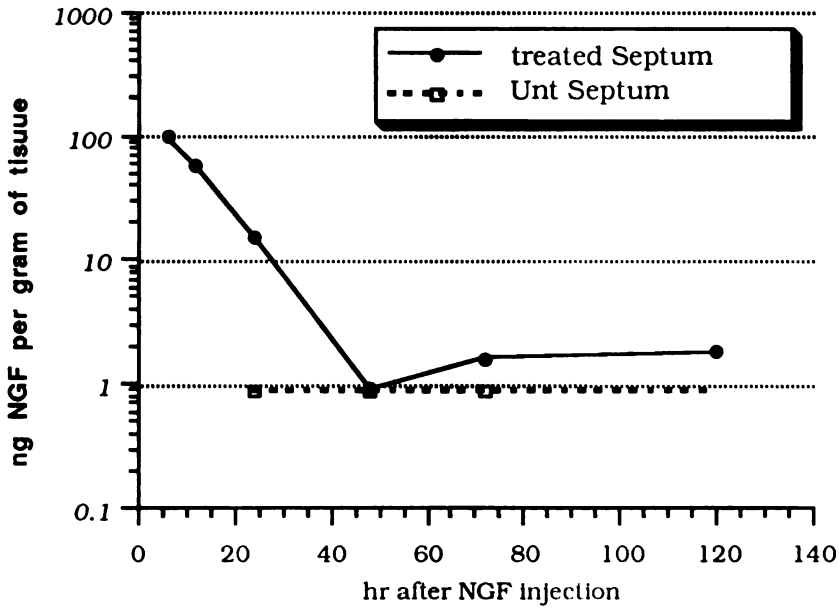

Figure 2.3 NGF clearance in the septum

2.2c Calculating the NGF clearance rate

Our plan was to place implants in hippocampus, therefore we calculated a clearance rate for this tissue. The clearance rate of NGF from the hippocampus was calculated using the formula:

$$\text{clearance rate} = \text{dose} / \text{area under the curve} \qquad (1)$$

$$= 30{,}000 \text{ ng} / 33920 \text{ ng/g (hr)}$$

$$= 0.9 \text{ g/hr}$$

where the dose was the amount of NGF administered through intraventricular injection and the area under the curve was calculated using Fig. 2.2 after NGF tissue level was extrapolated to time 0.

2.2d Rate of NGF delivery

The rate of delivery was calculated by multiplying the clearance rate by the desired tissue concentration. We defined a supraphysiologic NGF level to be at least 10 ng/g, a level 10 times the baseline in the adult hippocampus (Auburger, et al., 1987). Thus,

$$\text{rate of delivery} = \text{clearance rate} \times \text{desired concentration} \quad (2)$$
$$= 0.9\ \text{g/hr} \times 10\ \text{ng/g}$$
$$= 9\ \text{ng/hr}$$

The amount of NGF that had to be incorporated into each implant was then calculated, assuming a constant rate of NGF release and complete NGF release from the polymer matrix.

$$\text{amount of NGF} = \text{rate of delivery} \times \text{time} \quad (3)$$
$$= 9\ \text{ng/h} \times 24\ \text{hrs/day} \times 28\ \text{days}$$
$$= 6{,}048\ \text{ng or } 6\ \mu\text{g NGF/implant}$$

The amount of NGF per implant was then used to calculate the total amount of NGF needed to produce a block of NGF polymer (from which individual implants were cut). The dimension of a block of polymer was 12 x 10 x 1 mm, a volume of 120 mm^3. Each individual implant had a dimension of 1 x 2 x 1 mm, a volume of 2 mm^3. Therefore, each block of polymer can be cut into 60 individual implants. The amount of NGF needed for each block of polymer was calculated as:

$$\text{amount of NGF/block of polymer} =$$
$$\text{number of implants/block} \times \text{amount of NGF/implant} \quad (4)$$

MIT LIBRARIES

= 60 x 6 μg

= 360 μg of NGF/block of polymer

2.3 Carrier protein

A carrier protein is recommended in the polymer delivery system to protect the protein of interest from denaturation, from sticking to the walls of the polymer, and to give the necessary bulk of material for producing the polymer pore network. In this study, the carrier protein chosen was a highly purified form of rat serum albumin (RSA, Sigma, St Louis, MO). This protein is present in normal rat cerebrospinal fluid (CSF) and would be expected to be well tolerated (Fishman, 1992).

2.4 Loading volume

In deciding how much carrier protein to incorporate into the polymer, Rhine et al (1980) recommended a protein loading volume that would be 30–50% of the total polymer weight. This volume has been shown to release 70-95% of the incorporated protein (Rhine, et al., 1980). First, we calculated the amount of carrier protein to be incorporated into 1 block of polymer. The glass mold used for casting the polymer block held a total volume of 2 ml. This volume produced the polymer block dimension mentioned in Section 2.2, formula 4. A 10% EVAc solution was used. The total polymer weight in a block of polymer was calculated to be 10% of 2 ml, which was 0.2 g.

In this study, two loading volumes, 30% and 40%, were used in the preparation of polymer blocks. At a loading volume of 30%, the amount of carrier protein needed was 30% of 0.2 g, which was 0.06 g RSA/block of polymer. For a loading volume of 40%, the amount of carrier protein needed was 0.08 g of RSA/block of polymer.

NGF in buffer (PBS/Acetic acid solution, pH 7.0) was sterilized by passage through .22 μm Millipore™ filters, and was mixed with RSA. The NGF-RSA solution was

MIT LIBRARY

then quick-frozen and lyophilized overnight. Control powder—RSA alone—was prepared by dissolving RSA in the same buffer as above. It was then then quick-frozen, and lyophilized overnight. See Appendix A for the Table of recipes of all the implants prepared for this study.

2.5 Particle size

Rhine et al (1980) had shown that particle sizes ranging from 75–250 μm allowed for release of almost all of the incorporated protein. In this study, a < 90-μm particle size with a loading volume of 30% was arbitrarily chosen first. Two particle size-loading volume combinations — < 180- and < 250-μm with 40% loading volume — were used later. Lyophilized NGF/RSA powder (1:170, w/w, 30% loading volume) was passed through a 90-μm sieve (Fisher), producing NGF_{90} powder. A second batch of lyophilized NGF/RSA powder (1:226, w/w, 40% loading volume) was passed through a 180- and a 250-μm sieve to produce NGF_{180} and NGF_{250} powders, respectively. Control powders (RSA alone) were sieved in the same manner to produce corresponding RSA_{90}, RSA_{180}, and RSA_{250} powders.

2.6 EVAc polymer implant preparation

EVAc copolymer pellets were washed extensively in 100% ethanol with constant stirring at room temperature. The washing procedure was carried out for 2–3 weeks, with the ethanol being changed every other day. Pellets were then dried under vacuum for at least 2 weeks. A 10% EVAc solution (weight/volume) was prepared using dichloromethane (Fisher) as the solvent. NGF_{90} or NGF_{180} or NGF_{250} or their corresponding RSA powders, were incorporated into the polymer solution by vortexing. The mixture was immediately casted into a frozen glass mold (-70°C), and allowed to

UMDNJ LIBRARY

freeze for 10 minutes. This procedure assured uniform dispersion of the protein particles in the polymer. The casted polymer was transferred to a metal rack and allowed to polymerize at -20°C for 2 days. The polymerized block was then dried under vacuum for another 2 days. Using a dissecting microscope, the polymer blocks were cut into 1 x 2 x 1 mm individual implants. These procedures yielded the following implants: NGF_{90}, NGF_{180}, NGF_{250}, RSA_{90}, RSA_{180} and RSA_{250}. Control blank polymer implants were prepared following the same procedure without the addition of powdered protein. The implants were stored in dessicator jars at 4°C until use.

2.7 In vitro and in vivo NGF release kinetics

2.7a In vitro release experiment

It was necessary to show that NGF was released from the implants and that the released material was biologically active. Three implants each of NGF_{90}, RSA_{90}, and blanks were placed in a 96-well plate, one implant per well. To each well was added 150 µl of artificial cerebrospinal fluid (CSF)—a solution containing 150 mM sodium, 3 mM potassium, 1.4 mM calcium, 0.8 mM magnesium, 1 mM phosphorus, and 155 mM chloride, pH 7.4. The plate was transferred to a 37°C incubator, and supernatants were collected every day for 7 days and every 4th day thereafter for 35 days. After collecting the samples, fresh artificial CSF was added. The supernatants were divided into two vials and stored frozen at -70°C. Half of the supernatant was prepared and assayed for its NGF content using ELISA (see Appendix B for sample preparation and ELISA protocol). The other half was assayed for NGF activity using the chick dorsal root ganglia (DRG) bioassay (see Section 2.8).

NGF_{90} implants released a burst of NGF that averaged 50 ng/day during the first 7 days. The amount decreased to an average of 15 ng/day in the next week. In the

UCSF LIBRARY

last 3 weeks of the experiment, the implants released an average of 3 ng/day (Figure 2.4). Note that the implants failed to release the desired concentration—at least 10 ng NGF/day for 28 days—in the last 3 weeks of the experiment. Supernatants from RSA_{90} and blank implants showed no reactivity in the ELISA assay.

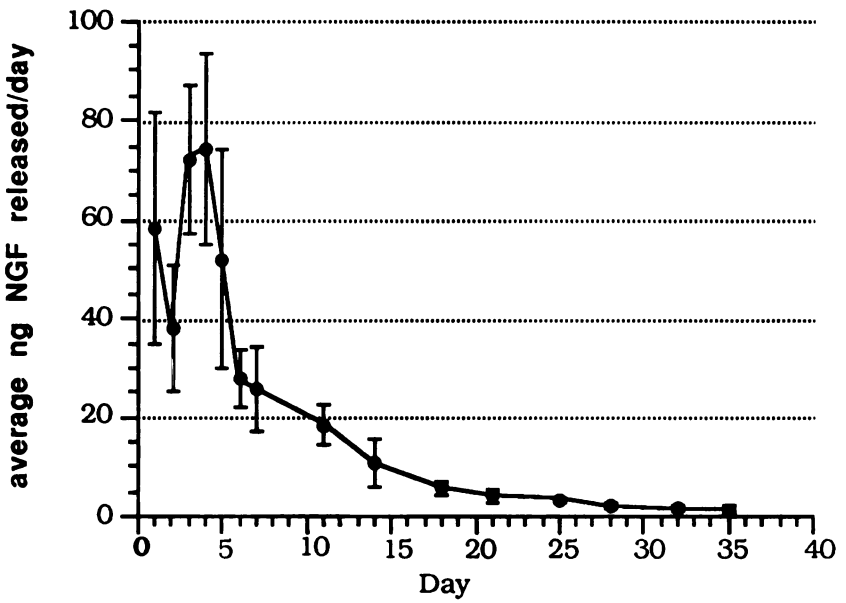

Figure 2.4 NGF released from three NGF90 implants in vitro

2.7b In vivo release experiment

Three NGF and three RSA implants were surgically placed into the right hippocampus of PD 2 rat pups using the procedure described in Section 3.4a. At 2, 4, 7, 12, 14, and 28 post-implantation day, the right and left septum and hippocampus were dissected and assayed for NGF levels using ELISA.

In vivo release results for NGF_{90} implants are shown in Figure 2.5. Note that NGF levels increased only on the side of implantation. The contralateral hippocampus showed NGF levels within normal range (~1 ng NGF/g). This suggests that NGF released from the implant did not diffuse widely but, instead, remained localized to the

UCSF LIBRARY

implanted hippocampus. At 14 days post-implantation, 7.6 ng NGF/g was measured in the right hippocampus; values of 5.6 ng/g, and 4.7 ng/g were measured at 21 and 28 days, respectively. A rate of NGF release was estimated by: 1) determining the fold increase over 1 ng/g at each time point measured; and 2) assuming that this level was also present in the period extending back in time to an earlier measured value or the beginning of the experiment. Though relatively crude, this estimate was useful for judging efficacy of NGF delivery. Using this method, NGF release from NGF_{90} implants led to levels that averaged 6.4 times the baseline level over 28 days.

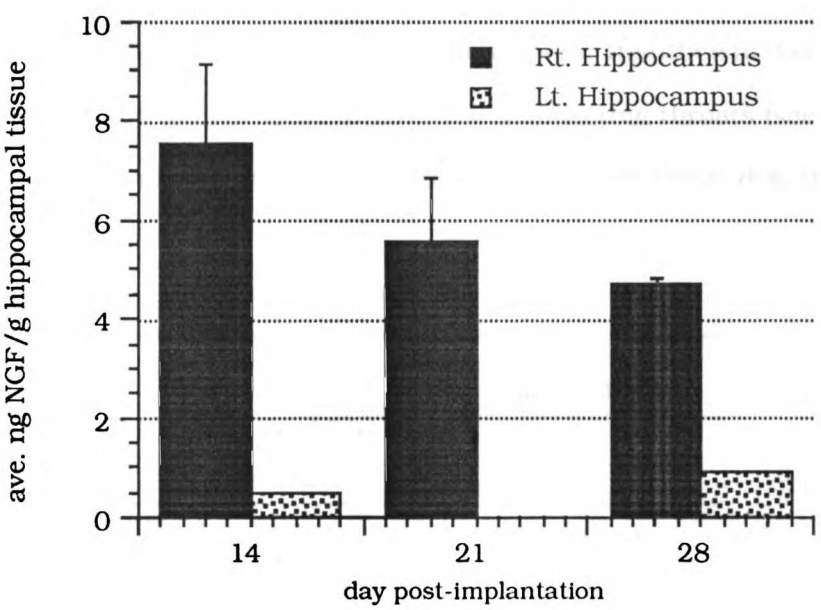

Figure 2.5 NGF released from three NGF90 implants in vivo, error bars represent standard deviation

The rather disappointing data for NGF levels using NGF_{90} implants predicted that cumulative NGF release was far less than anticipated. Cumulative NGF release could be calculated using the in vitro release data (Section 2.7a). These values are expressed as cumulative ng NGF released in Figure 2.6 and as cumulative percent of incorporated NGF released in Figure 2.7. From 361 to 538 ng NGF was released over 35

days (Fig. 2.6). These amounts, constituted only 6-9% of the total NGF incorporated (Fig. 2.7). Thus, ninety percent of the NGF was unaccounted for. To ask whether this was due to NGF being trapped inside the polymer implant, a simple experiment was done. The implants used in the in vitro release experiment, which had already released NGF for 35 days, were cut into 2 or 4 pieces and the pieces were placed into artificial CSF to test for additional in vitro release. Supernantants were collected at 1, 3, 5, and 7 days and assayed for NGF using the ELISA. The results of this experiment showed that an additional 1% to 1.6% of NGF was released over 7 days. These results confirmed the suspicion that NGF was trapped inside the implant. Trapping could be due to too small a particle size, insufficient loading volume or both. Too small a particle size can lead to the protein particles forming isolated individual pores. Insufficient loading volume, could cause pores to be too far apart to form interconnecting throats (see Section 2.1). These factors may explain the incomplete release of NGF from the NGF_{90} implants.

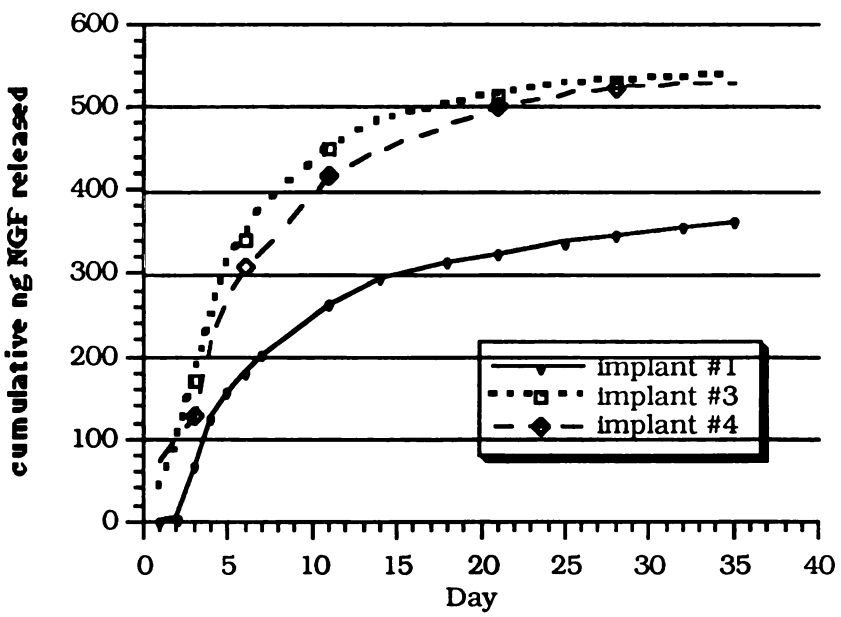

Figure 2.6 Cumulative NGF release from NGF90 implants

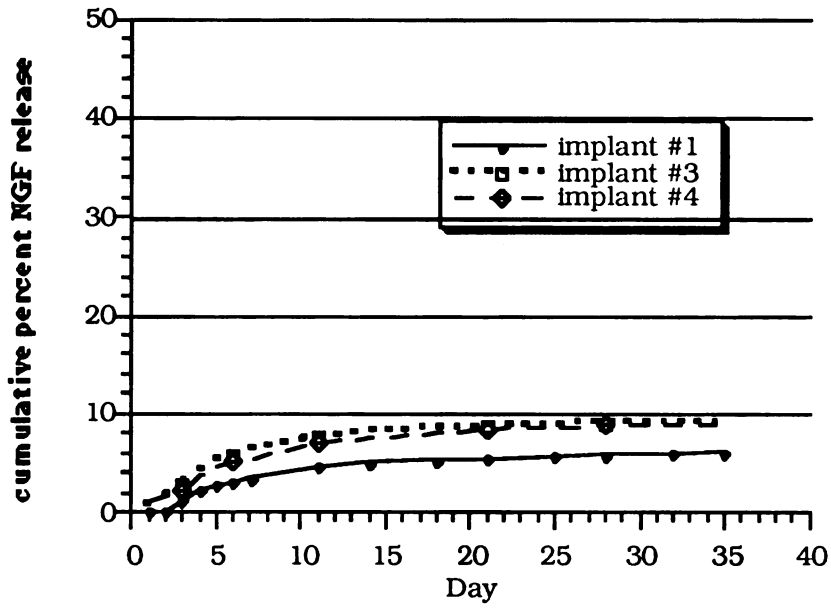

Figure 2.7 Cumulative percent NGF release from NGF90 implants

If the above explanation is correct, then increasing the particle size of the protein/carrier powder to 180 μm and 250 μm, and increasing the loading volume to 40% of total polymer weight should correct the problem of incomplete NGF release. For this reason, NGF_{180} and NGF_{250} implants were prepared following the same procedure as for NGF_{90} described in Sections 2.4 and 2.5. In vitro release experiments were carried out as described earlier with the exception of the sample collection scheme. Supernatants were collected every 4th day starting at day 2 for 26 days for a total of 7 time points.

Release kinetics from NGF_{180} and NGF_{250} implants in vitro are presented in Figures 2.8 and 2.9, respectively. Like NGF_{90}, both NGF_{180} and NGF_{250} showed an initial spurt of NGF release. However, NGF_{180} and NGF_{250} released far more NGF than NGF_{90}. In the first two days, about 37% (1.1 μg/day) of the total NGF incorporated was released by NGF_{180} and 70% (4 μg/day) by NGF_{250}. The rate of release gradually decreased to 13.4 ng/day for NGF_{180} and 28.2 ng/day for NGF_{250} by day 26.

Supernatants from RSA_{180}, RSA_{250}, and blank implants showed no NGF immunoreactivity in the ELISA.

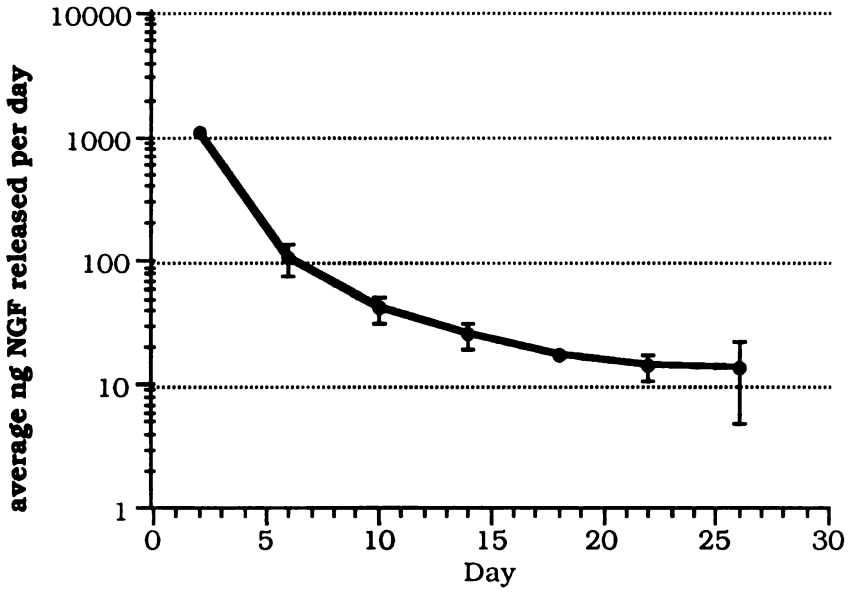

Figure 2.8 NGF released from three NGF180 implants in vitro

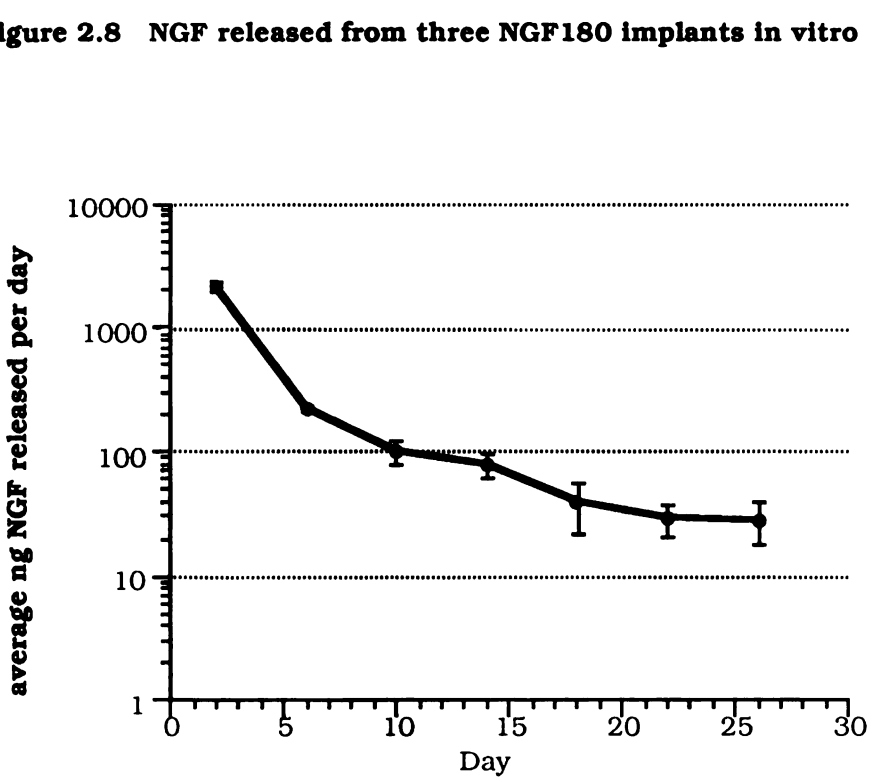

Figure 2.9 NGF released from three NGF250 implants in vitro

NGF_{250} was picked as the implant of choice. In vivo release of NGF_{250} was then examined following the same protocol as described earlier except that one implant was placed on each side of the hippocampus.

Figure 2.10 shows NGF levels in the hippocampus of animals treated with NGF implants. During the first week, NGF levels approximately 40-fold normal (i.e. untreated) were detected. Over the 28-day period, there was an average 13-fold increase in NGF levels relative to untreated animals. Note that in RSA-treated animals, endogenous NGF in the hippocampus increased 2.9-fold relative to untreated animals over the 28-day period. Whether this increase was due to injury caused by the surgical procedure or caused by RSA release into the brain was not ascertained. Of note, no NGF was detected in the hippocampus of RSA implanted rats in the first week, suggesting that these implants did not increase NGF levels during this period.

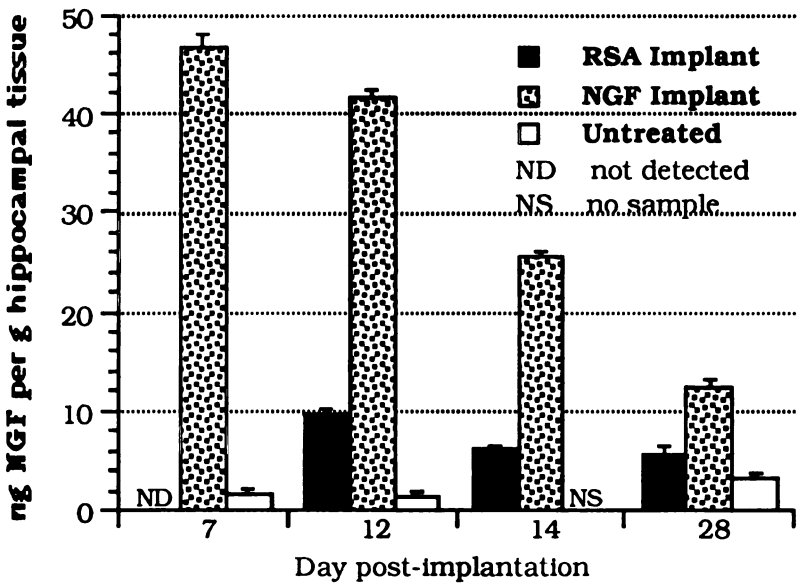

Figure 2.10 NGF levels in the hippocampus of brains that received implants at PD 1, error bars = sem (n = 3)

Given the ready diffusability of NGF in the CNS, production of supraphysiologic levels of NGF in the hippocampus would be expected to significantly increase the

availability of this factor to axons of BFCNs. Figure 2.11 shows data in support of this assertion. NGF_{250} placed in the right and left hippocampus resulted an average 10-fold increase in NGF levels in the septum over a 28-day period. Remarkably, at 7 days post-implantation, NGF levels in the septum was more than 30 ng/g. Of note, RSA treatment also increased septal NGF levels somewhat (1.2-fold increase over 28 days compared to untreated).

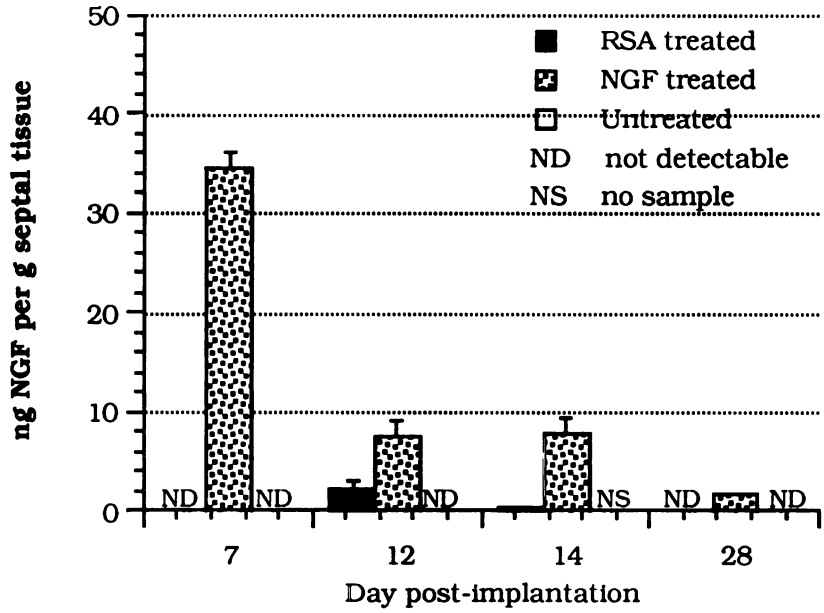

Figure 2.11 NGF levels in the septum of brains that received implants at PD 1, errer bars = sem (n = 3)

2.8 Bioactivity of NGF released from implants

The NGF released from implants in vitro was tested for bioactivity using the chick dorsal root ganglia bioassay (for detailed DRG protocol, see Appendix C). Dissociated embryonic neurons from the DRG respond to NGF with enhanced survival

and by growing neurites. The bioassay was set up so that a standard NGF bioactivity curve could be generated by treating ganglionic cells with a series of NGF concentrations. Supernatants from the implants, which had a known amount of immunoreactive NGF (from ELISA), were plated at a specific NGF concentration (100 pg/ml). After 24 hours, cells that grew neurites were counted and a standard curve generated. The number of cells that grew neurites in the sample wells were compared with the standard and the bioactivity was expressed as percent of the 100 pg NGF standard.

Figure 2.12 shows supernatants collected from the same implant at different days. The supernatants exhibited an average of 128% of the 100 pg NGF standard. Supernatants collected from RSA and blank implants exhibited 5% and 2% levels of the 100 pg standard, respectively, as shown in figure 2.13. These results confirmed that NGF released from the implants was fully active at the beginning (Day 3) of the experiments and remained bioactive during the later stages of the experiment.

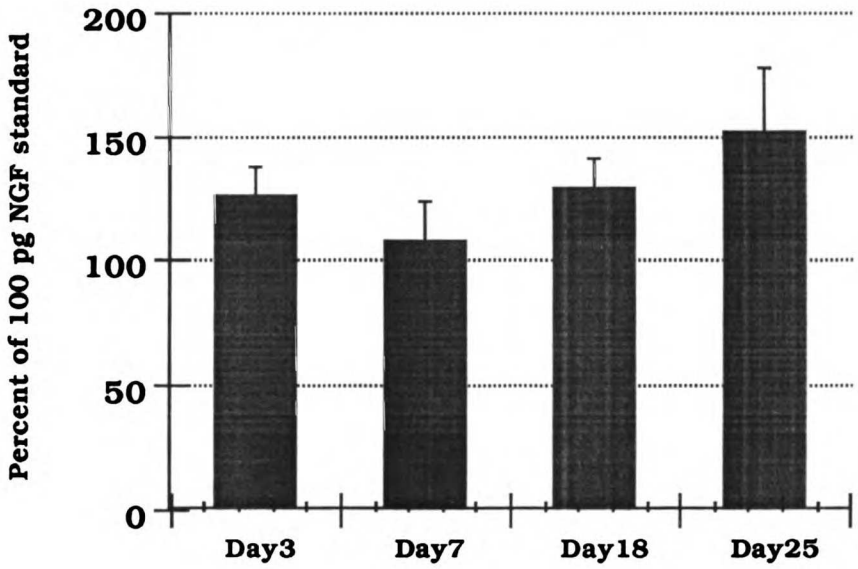

Figure 2.12 Bioactivity of NGF Released from Polymer Implants as Measured in DRG Assays, error bars = sd

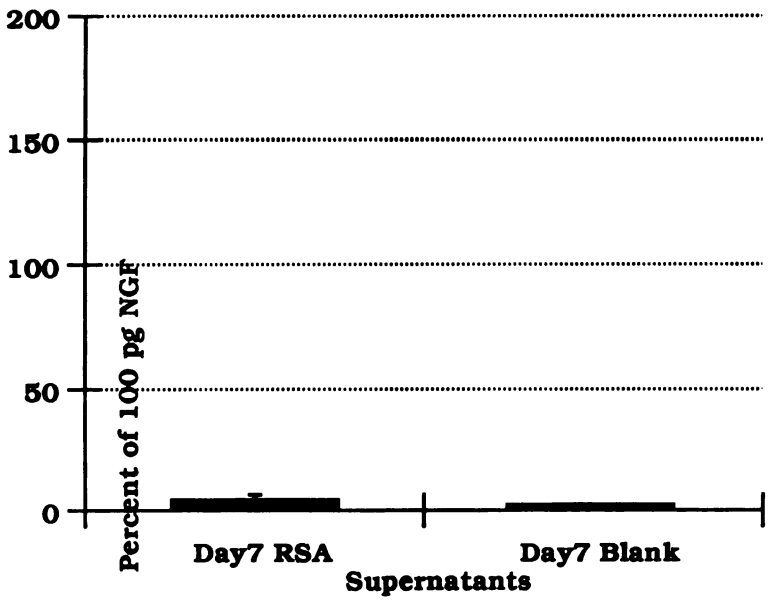

Figure 2.13 Bioactivity of supernatants from RSA and blank implants, error bars represent standadr deviation

Chapter 3

LONG TERM NGF TREATMENT AND ITS EFFECTS ON DEVELOPING SEPTAL CHOLINERGIC NEURONS

3.1 Hypothesis and Rationale

NGF is a neurotrophic factor for forebrain cholinergic neurons. If these cells compete for limited quantities of target-derived NGF for their survival during development, then administering NGF to achieve supraphysiologic levels should abort this process and result in an increased number of BFCNs.

3.2 Experimental Design

As discussed in chapter 1, developmental death of basal BFCNs can be predicted to begin at PD 0, and to continue for the next several days. In planning our studies, we reasoned that NGF should be adminstered during this period. Uncertainty regarding the timing of the cell death period encouraged us to extend the period of NGF administration to the last possible time for occurrence of developmental events. For BFCNs this is approximately PD 30. Thus, we administered NGF to rat pups to cover the entire first postnatal month.

NGF or RSA implants were surgically placed into each hippocampus of PD 1 rat pups according to the procedure described in Section 3.4. Hereafter, we will designate these animals as belonging to the NGF or the RSA groups. Control pups were unoperated at PD 1 and received no treatment; they will be designated as the untreated group. Implants were left in the brain for 28 days. BFCNs respond to exogenous NGF by increasing ChAT immunoreactivity and cell size. Both these measures could influence the ability to detect, and therefore count, BFCNs. It was necessary to devise a means to

avoid a bias between the NGF-treated group and the non-NGF-treated groups, so that they could be compared. The simplest solution was to give NGF at the end of the experiment so as to enhance the ChAT immunoreactivity and increase BFCN size in both groups. Vehicle was given to control for the NGF administration. Thus, on the 29th day post-implantation (i.e. at PD 29), either NGF (5 μg NGF/day in artificial CSF) or vehicle (artificial CSF alone) was given to each rat through an osmotic pump for an additional 6 days in all 3 treatment groups (see Figure 3.1 for the schematic experimental design). Therefore, there was a total of 7 treatment groups: 1) group one – animals received NGF implants and were then given either additional NGF through the pump (group 1A—NGF/NGF) or vehicle alone through the pump (group 1B—NGF/VEH); 2) group two – animals received RSA implants and were then given either NGF (group 2A—RSA/NGF) or vehicle (group 2B—RSA/VEH); and 3) group three – untreated animals either remained untreated throughout the 35-day experiment (group 3A—UNT/UNT), were given NGF (group 3B—UNT/NGF), or vehicle for the last 6 days of the experiment (group 3C—UNT/VEH).

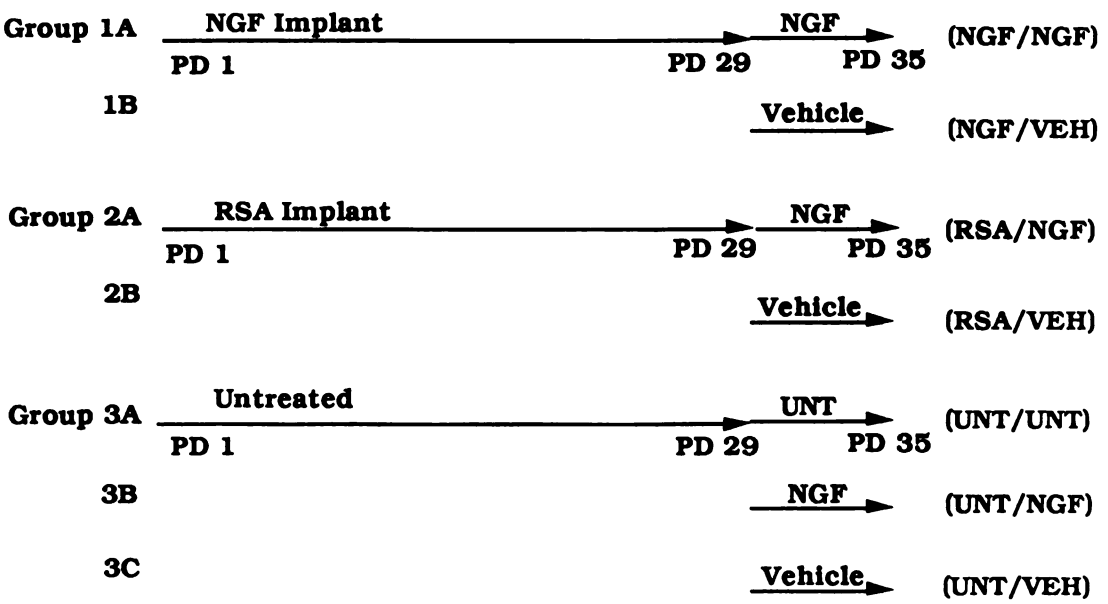

Figure 3.1. Experimental Design.

3.3 Experimental Materials

Neonatal Sprague/Dawley rats belonging to a natural litter were used. The mother nursed the litter until the pups were weaned at PD 29. The animals were purchased from Bantin and Kingman, Richmond, California.

NGF_{250} and RSA_{250} implants were prepared as described in Sections 2.6 and 2.7. The NGF implants were designed to deliver at least 10 ng of NGF/g of hippocampal tissue/day for 28 days. RSA implants were used as the control.

NGF was prepared from mouse submaxillary glands according to the method of Mobley et al (1986). For loading into osmotic pumps, NGF was sterilized by passage through .22 μm Millipore™ filters, lyophilized overnight, and dissolved in sterile artificial CSF. ALZET mini osmotic pumps (model 7D), and brain infusion kits were purchased from Alza, Inc. Palo Alto, California.

3.4 Experimental Methods

3.4a Implant placement surgery

Anesthesia was carried out by chilling the rat pup in a $-20^{o}C$ freezer for 10 minutes. The anesthetized pup was then transferred onto a surgical stage overlying a base of ice. The dorsal surface of the head was cleaned with 70% ethanol. With a #15 scalpel, a 1/2-inch incision was made along the midline of the head. The incision wound was carefully retracted with the left thumb and index fingers while the remaining fingers stabilized the head. The location for the implant was then determined. The superior sagittal sinus is clearly visible in the midline and bifurcates caudally into the right and left transverse or lateral sinuses. The implant was placed approximately 1.0 mm rostral to the transverse sinus and approximately 1.2 mm lateral to the superior sagittal sinus. A skull flap was made using a #15 scalpel for the first cut.

Microsurgical scissors were used to complete the flap. The flap was carefully reflected toward the midline. A small cut was then made in the cortex where the implant was to be placed with the same scissors. Using a pair of microsurgical forceps, one end of the rectangular implant was picked up, dipped into a pen-strep solution (10,000 units/ml penicillin "G" and 10,000 µg/ml streptomycin sulfate), patted on a sterile gauze, and very carefully lowered into the cortex so that the edge of the implant was flush with the surface of the cortex. This positioned the implant so that one end sat on the dorsal edge of the hippocampus and the other end abutted the dorsal surface of the cortex. The skull flap was then replaced. Another implant was placed on the opposite side using the same procedure.

The surgical area was patted dry with a sterile cotton swab and the incision closed with a single surgeon's knot using 5-0 silk sutures. The rest of the wound was closed by applying Krazy glue along the incision. The pup was revived by gentle warming on a heating pad until fully awake and was then returned to the mother. There were no apparent adverse consequences of the procedure. Pups were observed to nurse normally immediately following recovery.

3.4b Osmotic pump placement surgery

Each infusion apparatus was assembled according to manufacturer's instructions using a cannula length of 4.5 mm and a catheter tube length of 3/4 inch. Krazy glue was used to adjust the cannula length and to stabilize the catheter tube to the cannula head and the pump flow regulator. The assembled infusion kits were gas sterilized prior to use.

On the day of surgery, sterile pumps were filled with either NGF (see NGF preparation above) or vehicle (artificial CSF alone) according to manufacturer's instructions and set aside in upright positions in a covered sterile dish until ready to be assembled with the infusion apparatus.

Anesthetic was prepared by adding 1.8 ml of ketamine HCL (100 mg/ml), 0.48 ml of xylazine (20 mg/ml), and 0.25 ml of acepromazine maleate (10 mg/ml) to 10 ml of injectable normal saline solution. From 0.25–0.30 ml of anesthetic solution was used to anesthetize each 29-day-old rat. The dorsum of the head was shaved and swabbed with 70% ethanol. The animal was then positioned on the stereotaxic surgical stage using the head positioning device. With a #15 scalpel, an incision 1/2–3/4 inch long was made along the midline of the head and a subcutaneous pouch was prepared which started from the caudal end of the incision towards the neck. The incision was retracted using the ear rods of the stereotaxic equipment to expose the skull. With a scalpel, the periosteum was scraped off to expose the bregma. A mark was made on the bregma. The position of the cannula was located stereotaxically at 0.4 to 0.5 mm rostral and 1.2 mm lateral to the bregma. Under the dissecting scope, a 0.5 mm hole was drilled at the mark, and through the skull using an electric hand drill (Dremel Moto-Tool Kit) with a #2 long round bur. Light, intermittent pressure was applied on the drill and skull. The hole was flushed with sterile PBS and any excess PBS and blood dabbed off with a cotton swab. At this point, the pump assembly prepared earlier was completed. The infusion apparatus was filled with either NGF or vehicle, with an extra drop of solution left at the tip of the flow regulator. It was carefully inserted into a corresponding NGF- or vehicle-filled pump. The pump/cannula assembly was secured by applying a thin layer of Krazy glue around the catheter-pump junction. The whole pump assembly was then carefully inserted into the subcutaneous pouch while keeping the cannula sterile. Using a pair of microsurgical forceps, the cannula was positioned directly above the hole in the skull with the cannula perpendicular to the horizontal axis of the head. A small drop of glue was placed on the skull adjacent to the hole and the cannula was carefully lowered into the hole. A small amount of dental methylmethacrylate was then applied at the cannula/skull junction to stabilize the pump assembly. The incision was

closed with 3-4 surgical clips. Animals were returned to their cage and recovered quickly without evidence of adverse effects from the surgery.

3.4c Brain processing

For infusion, the animal was anesthetized with 0.5 ml pentobarbital sodium (50 mg/ml) and the thoracic cavity opened to expose the heart. A puncture was made in the right atrium and 50-80 ml of cold PBS was introduced directly into the left ventricle through a #27 butterfly needle connected to a pump set to deliver 10ml of fluid per minute. The procedure was completed by giving 150 ml of 4% paraformaldehyde in 0.1 M phosphate buffer, pH 7.4. The brain was carefully removed and post-fixed in the same paraformaldehyde solution for 4–12 hours. Cryoprotection was carried out in 20% sucrose in 0.1 M phosphate buffer for 24–36 hours. The brain was quick frozen in pulverized dry ice and stored at -70^{o}C until ready for cutting and staining.

For sectioning, the frozen whole brain was laid on a flat glass plate so that the ventral surface touched the glass. A straight up and down cut was made to remove the hindbrain (cerebellum and brain stem). The forebrain was then mounted onto the stage of the freezing–sliding microtome using TBS (20 mM Tris, 150 mM NaCL, pH 7.4). The long axis of the forebrain was positioned perpendicular to the stage. Coronal sections were then cut at 40 µm thickness and the sections kept floating in buffer. The rostral anatomical boundary for the MSN was the meeting of the genu of the corpus collosum medially; the caudal boundary was the meeting of the right and left anterior comissures at the midline. Sections constituting the entire MSN were collected and immunostained for ChAT, a selective marker for cholinergic neurons. Hippocampal sections were also collected and histochemically stained for acetylcholinesterase (AChE), a marker for cholinergic fibers.

For immunostaining, endogenous peroxidase was quenched with 1% H_2O_2 in TBS for 15 minutes. Sections were pre-blocked with 5% normal rabbit serum (NRS) in

TBST (TBS with 0.3% Triton x 100) for 30 minutes at room temperature. The samples were then incubated for 12 hours at 4°C in primary antibody solution—1:2000 of goat anti-ChAT (Chemicon) in TBST with 1% NRS. The sections were washed extensively in TBS and incubated for 1 hour at room temperature in the secondary antibody solution—1:500 of biotinylated rabbit ant-goat IgG (Vector) in TBST. The sections were again washed in TBS and incubated for 1 hour at room temperature in Vectastain ABC *Elite* reagent (Vector) (1:400 each of reagent A and B in TBS). Color development was carried out by incubating the sections in 0.05% 3,3'diaminobenzidine (Sigma) solution with 0.01% H_2O_2 for 5–30 minutes. The sections were then mounted in their appropriate order on glass slides and coverslipped.

For AChE histochemistry, frozen sections were incubated in a substrate solution —0.02 M acetyl thiocholine iodide (Sigma) in Tris maleate buffer, pH 5.7, containing 5 mM sodium citrate, 3 mM copper sulfate, and 0.5 mM potassium ferricyanide—for 2 hours or until the reaction product (copper ferrocyanide) became visible. The sections were then mounted on slides and coverslipped.

3.4d Stereology

In this study, we elected to use an unbiased stereological method to estimate MSN neuron numbers. The optical disector is a three-dimensional stereological probe that provides an accurate estimate of neuronal number without the methodological assumptions of conventional techniques concerning the size, shape, and orientation of the objects being counted. Forty-micron brain sections were used. At this thickness, neurons containing a nucleus and a nucleolus can only be in one section regardless of its size, shape and orientation. By using microscope objectives with high numerical aperture, it is possible to optically section through the thickness of the section and only count the neurons with the appropriate specifications. Thus, a neuron can only be counted once in an unbiased manner (West, 1993, Mouton, et al., 1994).

The basic stereological equipment consisted of a Leitz Aristoplan microscope connected to a video screen through a black and white video camera. A point grid and an unbiased disector frame drawn on sheets of transparencies were superimposed and taped onto the video screen. The grid was used to estimate the volume of the MSN according to Cavalieri's method (Cavalieri, 1966), while the disector frame was used to estimate cell number employing the optical disector method (Gunderson, 1986). Movement of the microscope stage in the X-Y direction as well as the Z-plane was accomplished manually. Using the grid system as a guide, the stage was moved from one field of view to the next in the X-Y direction. Movement along the Z-plane was accomplished by turning the fine focus knob up and down the thickness of the section. The latter was carried out by first focusing on an anatomic structure, e.g. a blood vessel, on the surface of the section and tracing it down to the bottom of the section.

Ten ChAT-stained sections were sampled uniformly with a random start, i.e., in a set of serially mounted sections belonging to one brain, the first section was picked randomly, followed by every fourth section thereafter. The reference space, containing the MSN, was determined in each section, and the boundaries were marked on the back of each slide. To accomplish this, each slide was placed under a 10 x dissecting microscope. Using a superfine marker, a line was drawn across the tops of the right and left anterior comissure, thus marking the ventral boundary of the reference space. Dorsally, the reference space extended to the top of the ChAT-positive cell population of the MSN. The lateral boundaries were drawn from the ventral to the dorsal boundary line and were placed so as to include at least 90% of the ChAT-positive neurons. Figure 3.2 shows the reference space of the MSN.

Each marked section was then placed on the microscope stage and the volume estimated using a Leica 2.5x/.8 NA objective. Employing point counting and the unbiased Cavalieri formula, the reference volume of the medial MSN was calculated as:

$$\text{Vol}_{(MSN)}\,(mm^3) = \Sigma P \bullet a\{p\} \bullet t \bullet k \qquad (5)$$

summed across all sections, where ΣP = the number of points falling within the outlined reference space on each section; a{p} = area per point in mm^2, corrected for areal magnification; t = thickness of the section in mm, as measured by estimating the distance between the top and bottom of the section along the z-axis; and k = period between each sampled section (every fourth section).

Figure 3.2 Reference space of the medial septal nuclues (MSN)

Cell number was estimated using the optical disector method under high resolution light microscopy with a Leica 100x/1.32 NA oil immersion objective. First, the disector frame (attached to the screen) was moved to a random starting point. A uniform pattern was used to move systematically through the reference space. A total of 100 to 200 disectors were counted through the entire MSN of each animal. All cells in which the nucleolus fell within the disector frame or touched the inclusion lines of the disector frame were counted. The numerical density (N_V) of ChAT-positive neurons in the MSN was calculated as:

N_V (cells/mm^3) = total ChAT-positive cells counted/(total number of disectors counted x volume of a single disector in mm^3) (6)

where the volume of a single disector = area of the disector frame in mm^2 x height of the disector = thickness of the section.

Using the results from equations (5) and (6), the total cell number was calculated as:

Total cell number = $Vol_{(MSN)}$ (mm^3) x N_V (cells/mm^3) (7)

Within-group (coefficient of variance, CV = SD/mean) and within-individual (coefficient of error, CE) variations were calculated as described (Gunderson and Jensen, 1987, West, et al., 1991). Between-group testing for statistical significance at the level of 0.05 was carried out using the two-tailed Student's t-test.

3.5 Results

Experimental animals recovered from surgeries without any apparent signs of adverse effects. Figure 3.3 shows the weight gain monitored through the experimental period for two representative litters.

The position of the implants in the hippocampus were found to be satisfactory as shown in the photomicrograph of an AChE-stained hippocampus (Figure 3.4). In all cases, the implants were in contact with the hippocampus. Slight deformations in the tissues were noted around the implant, evidently caused by the surgical procedure. However, the intensity of cholinergic fiber staining was the same as in an untreated hippocampus, pointing to normal pattern for arborization of cholinergic fibers in the hippocampus and suggesting the presence of normal levels of AChE within these fibers.

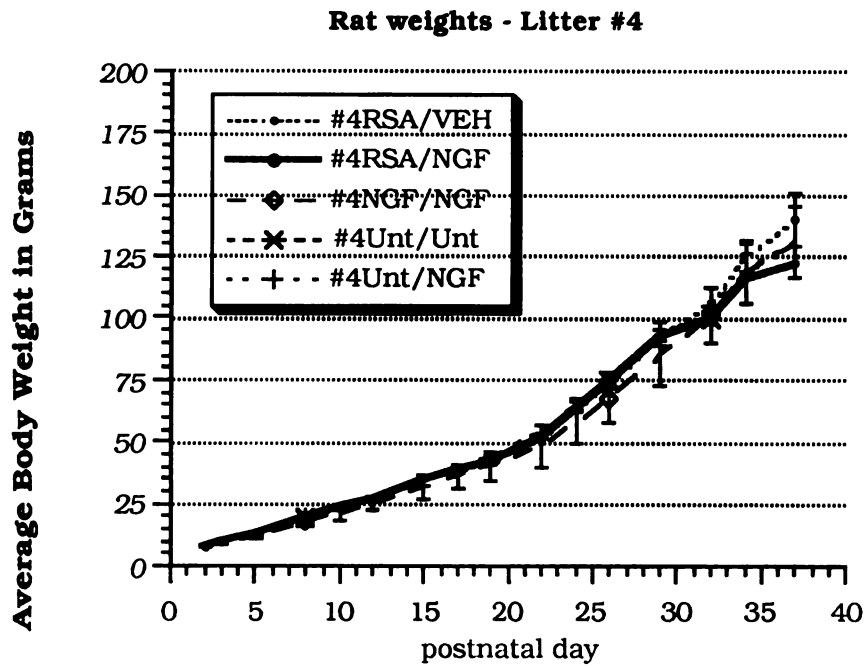

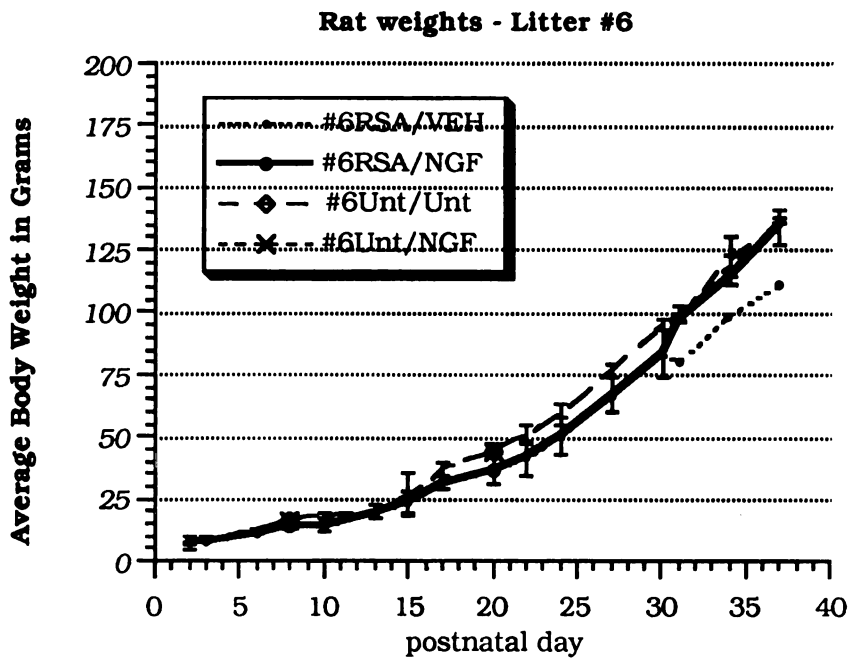

Figure 3.3 Weight gain of experimental animals (from litters #4 & #6) monitored through the entire duration of the experiment

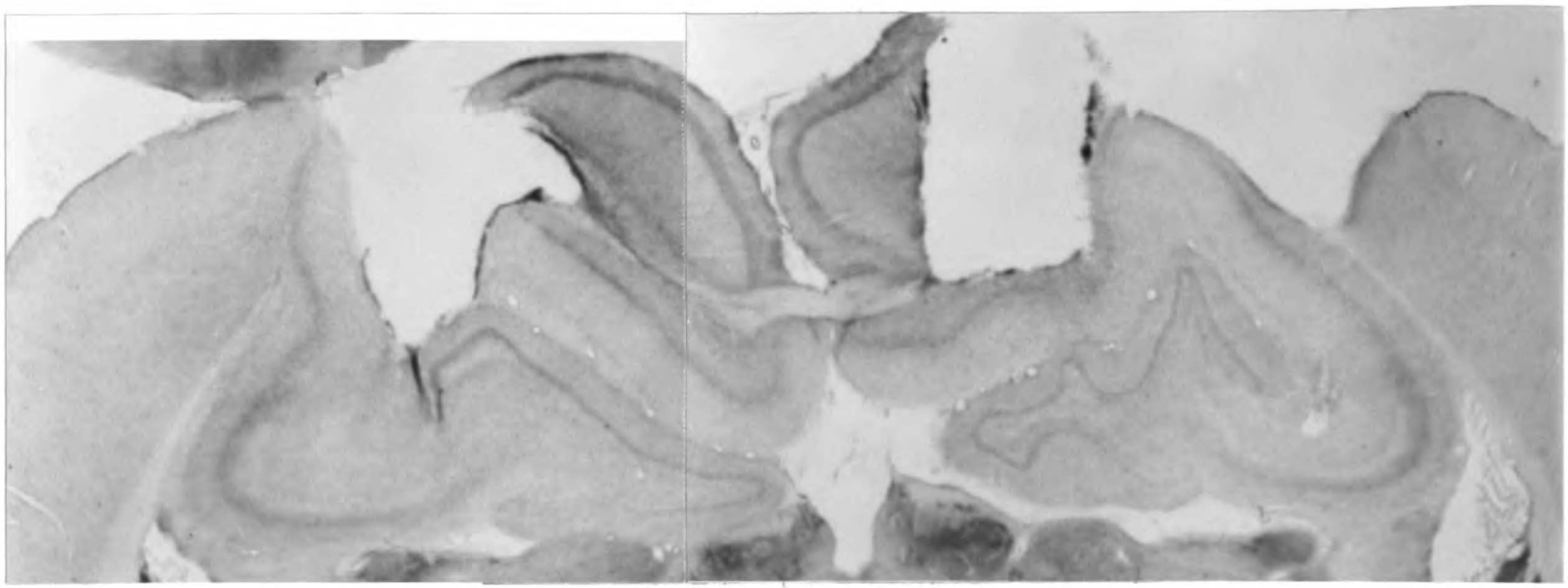

Figure 3.4 AChE-stained hippocampus showing the position of the implants, 220 x magnification

Figure 3.5 shows a representative photomicrograph of the residual tract created by the cannula of the osmotic pump assembly. In all cases, the cannulae were positioned within the ventricular space.

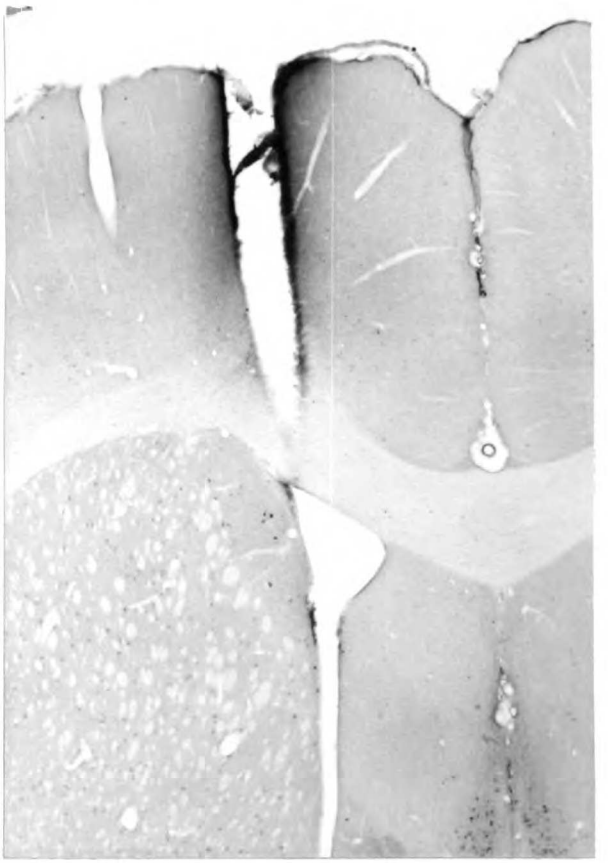

Figure 3.5 Position of the cannula in the lateral cerebral ventricular space

ChAT-immunostained brain sections containing the MSN showing pronounced and specific staining of cholinergic neurons. Figures 3.6 A & B show representative brain sections.

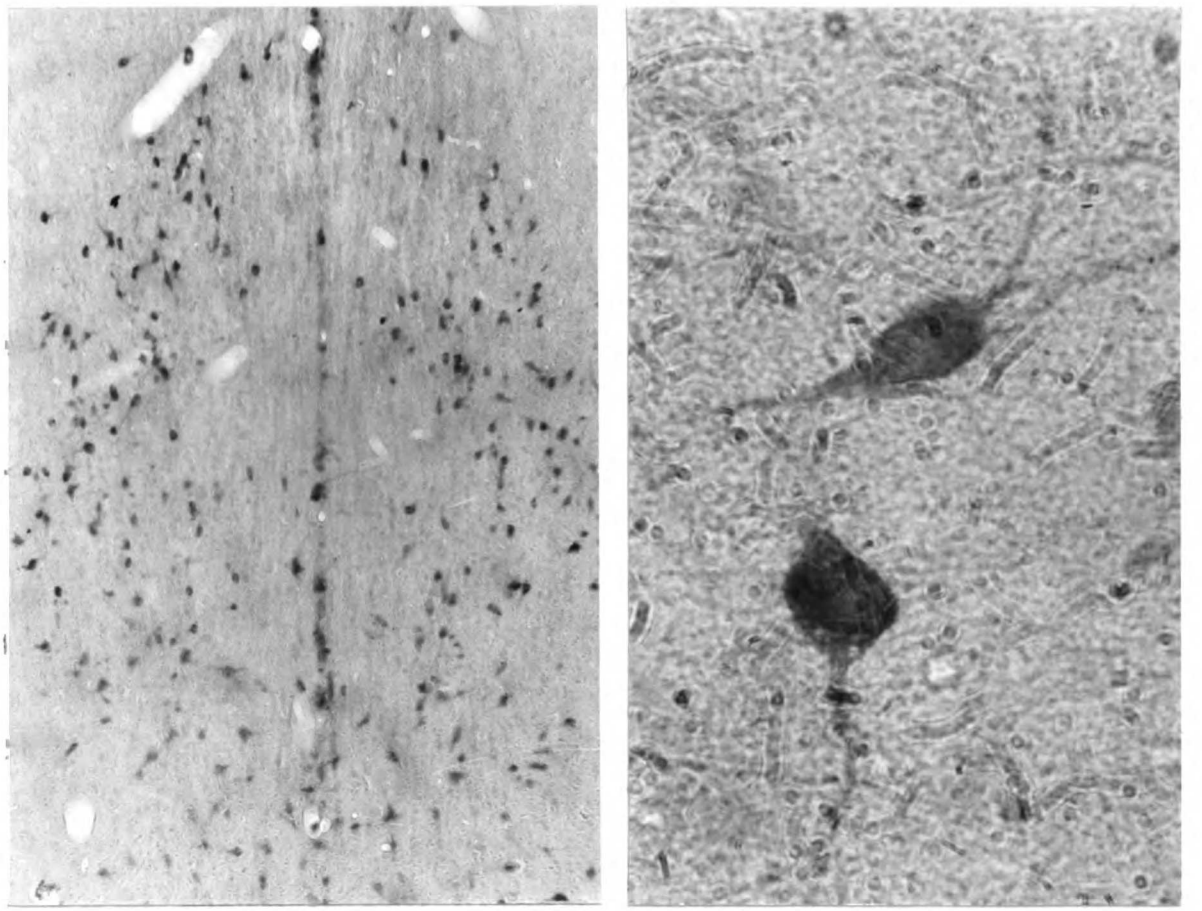

Figure 3.6 A & B ChAT-immunostained MSN section
A (left) 3500 x magnification, and
B (right) 8700 x magnification

Using unbiased stereological methods, the number of ChAT-positive neurons in the medial septum in all treatment groups were estimated and compared. Figure 3.7 presents the results plotted as scatter (symbols) and bar graphs. The bars represent the group average per treatment group with the standard error of the mean.

When exogenous NGF was given to previously untreated animals at PD 29, there was a 33% increase in the number of ChAT-positive neurons in the MSN (UNT/UNT vs UNT/NGF, $p = 0.016$). Giving vehicle alone (UNT/VEH) resulted in a small increase in the number of ChAT-positive neurons as compared to untreated animals (UNT/UNT), but the increase was not significant ($p = 0.144$). The increase in ChAT-positive neurons is unlikely to be due to a true increase in the number of cholinergic neurons. It most likely represents an increase in the ability to detect cholinergic neurons that results from the increase in ChAT protein immunostaining and BFCN cell size brought about by NGF treatment. The same increase in number has been detected following NGF treatment of adult rats (D. Holtzman,Y. Li and W. Mobley personal communication).

To isolate the effect of the implant surgery on the number of ChAT-positive neurons, the UNT/VEH group was compared with the RSA/VEH group. In the animals that received RSA implants, there was a 31% decrease ($p = 0.003$) in ChAT-positive neurons. This suggests that the surgery reduced the number of this cell population, perhaps as a result of injury during the procedure. However, the surgery-related change did not cause neurons to lose their ability to respond to exogenous NGF. There was a 28% increase in the number of ChAT-positive neurons in the RSA/NGF group when compared to the RSA/VEH group ($p = 0.006$). Indeed, this change was approximately equal to that seen between UNT/UNT and UNT/NGF.

The effect of prolonged NGF treatment on developing cholinergic neurons was examined by comparing the NGF/NGF group with the RSA/NGF group. The numbers of ChAT-positive cholinergic neurons in the MSN of these two treatment groups were not different ($p = 0.778$). These data indicate that NGF did not increase ChAT-positive cell number and they are evidence against the hypothesis that increasing the level of NGF in the target of these cells can rescue them from developmental death. Tables 2 and 3 summarize the results for the 7 treatment groups.

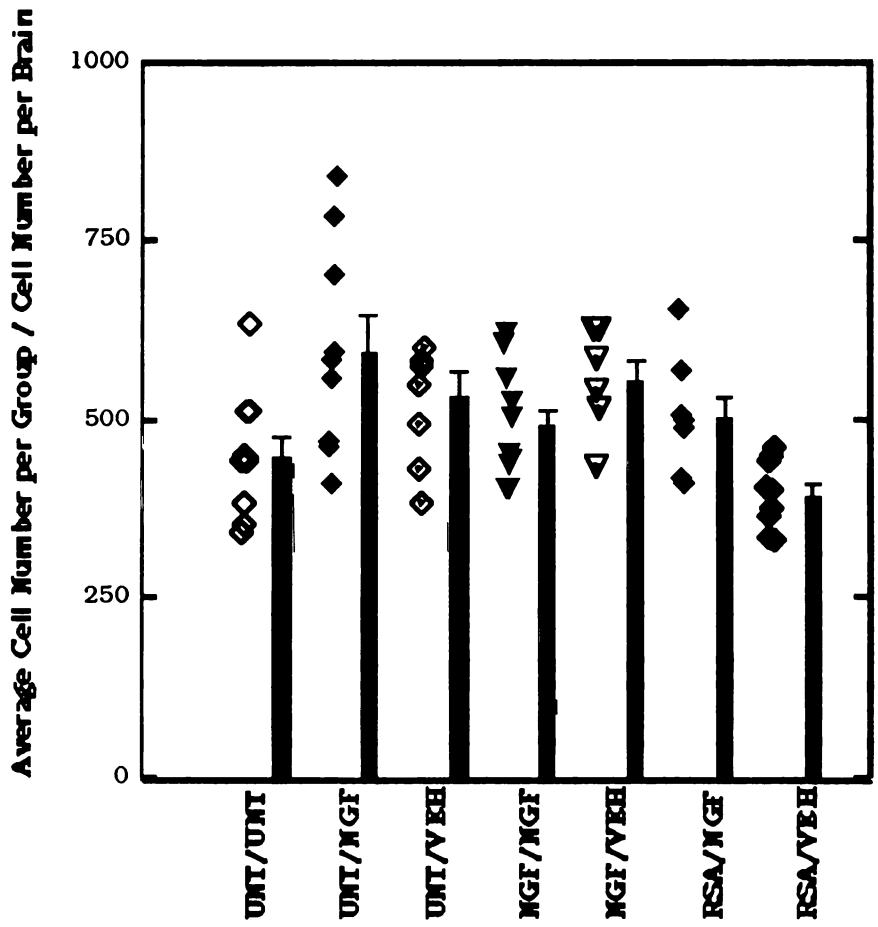

Figure 3.6 Effect of long-term NGF treatment on developing septal cholinergic neurons

Table 3 Summary of results

Rat #	UNT/UNT	UNT/NGF	UNT/VEH	NGF/NGF	NGF/VEH	RSA/NGF	RSA/VEH
1	440	467	549	602	627	652	404
2	341	457	428	617	433	565	361
3	380	407	490	400	540	413	440
4	350	555	574	554	585	503	332
5	447	580	582	449	624	486	399
6	442	591	379	434	515	495	375
7	512	782	600	398		408	446
8	441	701		501			459
9	632	837		439			330
10	509			521			
Mean	**449**	**597**	**515**	**492**	**554**	**503**	**394**
SEM	**27.4**	**49.6**	**29.9**	**25.3**	**30.3**	**32.2**	**16.1**
CE	**6.11**	**5.57**	**6.94**	**6.35**	**7.68**	**5.97**	**6.13**
CV	**0.19**	**0.25**	**0.16**	**0.16**	**0.13**	**0.17**	**0.12**
BV	**6.11**	**5.57**	**6.94**	**6.35**	**7.70**	**5.98**	**6.13**

CE (coefficient of error) or error variance, estimates within sample variation, which includes method error and biological variation within each sample/brain.
CV (coefficient of variance) or the observed variance, estimates between sample variation.
BV (biological variance)
SEM (standard error of the mean)

Table 4 Summary of significance of group differences

Groups tested	statistical significance	p value
UNT/UNT vs UNT/NGF	S	0.016
UNT/UNT vs UNT/VEH	NS	0.144
UNT/VEH vs RSA/VEH	S	0.003
RSA/VEH vs RSA/NGF	S	0.006
NGF/NGF vs RSA/NGF	NS	0.778

3.6 Conclusion

We asked if markedly increasing NGF levels in the hippocampus from PD 1 through PD 29 would result in increased survival of BFCNs registered as increase in the number of cholinergic neurons in the MSN. The results showed no effect of NGF on cholinergic neuron number.

Chapter 4

DISCUSSION

4.1 Long-term NGF treatment did not rescue septal cholinergic neurons from developmental cell death

Marked increases in NGF failed to result in an increased number of septal BFCNs. This result argues that NGF does not support survival of BFCNs in the postnatal period. However, there are several alternative explanations. They include: 1) BFCNs do not undergo cell death during development; 2) BFCNs do undergo developmental death but do so before PD 1, i.e. prior to the arrival of their axons in the target and to our NGF treatment; and 3) BFCN death occurs at the time predicted and is influenced by NGF, but the normal tissue levels of endogenous NGF are sufficient to ensure survival of all these cells. Definitive data for whether and when BFCNs die during development will be required to resolve these issues. We, however, can say that if developing BFCNs die, target-derived NGF does not appear to be limiting for their survival.

Naturally occurring cell death in normal development is as fundamental a process as growth and differentiation. Its occurrence is widespread throughout ontogeny. Phylogenetic degeneration causes the involution of vestigial and larval organs; morphogenetic degeneration results in changes that bring about mature forms of tissues and organs; and histogenetic degeneration leads to differentiation of tissues (Server and Mobley, 1991). Data from cell death studies point to naturally occurring death as an autonomous, gene-directed event (Server and Mobley, 1991, Williams and Smith, 1993). The presence or absence of growth factors or neurotrophic factors in the immediate environment of a cell has a marked influence on whether cells live or die. In

the PNS, neuron death in the developing peripheral ganglia, e.g. the DRG, SCG and TG, is well documented. A role for NGF in regulating survival of these neurons has been shown (Davies, et al., 1987, Wright, et al., 1983). Sequestration of NGF via antibody administration resulted in almost complete destruction of sympathetic neurons; whereas, NGF treatment resulted in overgrowth of sensory and sympathetic ganglia and excessive production of neurites (Levi-Montalcini and Booker, 1960, Levi-Montalcini and Cohen, 1956). We attempted to translate these findings to the CNS. Our study showed that NGF had no apparent effect on the survival of BFCNs. Several suggestions arise from this observation.

First, it is possible that developmental death does not occur among septal BFCNs. Cell death is widespread in the developing nervous system and most neuronal populations in the PNS and CNS demonstrate considerable loss of cells. The numerical matching of neurons and their targets is presumed to be the goal of developmental death (Cowan, 1984). BFCNs are projection neurons and their pattern of innervation in the hippocampus is stereotypic and highly organized. Thus, like NGF-responsive PNS neurons, one would expect that neuron-target matching would also be important for these cells and that developmental cell death would characterize this population. It is conceivable that neuron-target matching is not important to this system and that the innervation of the hippocampal target is not tightly regulated. However, there is evidence in neonatal rats that the target is important for cell survival in that its ablation does result in the loss of developing BFCNs (Burke, et al., 1995, Sofroniew, et al., 1993). Though these data cannot be directly extrapolated to the uninjured hippocampus, it is most likely that the hippocampal target is matched to innervating BFCNs and that developmental death does characterize this population. Proof of this assertion will require additional studies. Fragmentation of DNA is one manifestation of programmed cell death. TUNEL (i.e. terminal dUTP nick end labeling) histochemistry is a method for marking cells undegoing cell death (Hedreen, et al., 1994, Wilcox and Kitt, 1994). This

method utilizes biotinylated dUTP to label broken DNA in the nucleus of dying cells. Use of TUNEL in developing basal forebrain would be useful for determining whether BFCNs die during development.

A second possibility for explaining our result is that developmental cell death of septal BFCNs does occur, but prior to BFCN axons contacting their target. This possibility would eliminate a regulatory role for the target. It would instead suggest that cell viability is regulated by the local trophic environment in the basal forebrain, or cues in the path over which BFCN axons grow, or an autonomous program running in BFCNs. It should be noted that even among PNS neurons, cell death can occur prior to target contact. Oppenheim and colleagues demonstrated cell death in large DRG neurons very soon after the last mitosis and well before target contact (Oppenheim, et al., 1990). Thus, the possibility must be entertained that for BFCN, death can occur prior to target contact. Trophic influences acting before target contact can be readily envisioned. It is certainly the case that trophic factors are present in neuronal nuclei (Schechter and Bothwell, 1981, Henderson, et al., 1993), and it has been argued that autocrine or paracrine presentation of neurotrophins would serve to regulate developmental neuron death (Schechter and Bothwell, 1981, Grimes, et al., 1993). It is equally possible that trophic factors are found along the pathways for axon growth. Indeed, in developing sciatic nerve, NGF is produced in supporting cells and this may provide a local source of NGF (Heumann, et al., 1987). Whether this source of NGF is important during initial axon outgrowth is uncertain, and we know of no data to indicate that this source regulates developmental death of NGF-responsive neurons. Of note, the recent discovery of diffusible, chemoattractant molecules raises the possibility that axon pathways are normally marked by such factors (Kennedy, et al., 1994, Serafini, et al., 1994, Kennedy and Tessier-Lavigne, 1995). Conceivably, some netrin-like factors could regulate survival. Indeed, NGF itself has been shown to be chemotropic both in vitro and in vivo (Longo, et al., 1993, Kennedy and Tessier-Lavigne,

1995). Finally, BFCN deaths could be controlled by genetic programs autonomously running in these cells. Davies et al (1994) have provided in vitro evidence that, the time when sensory neurons acquire neurotrophin independence and their axonal outgrowth rate is correlated with their target distance. This suggests that these neurons possess an intrinsic clock that switches on at the right time in accordance with the time it normally takes their axons to reach their targets. Although these data are best understood in the setting of target-regulated events, they do suggest that developing neurons are programmed to die via a mechanism whose activation is independent of target contact. A consideration related to this discussion is that cell death occurs virtually immediately upon target contact and is completed very rapidly. In this case the period of BFCN death would end essentially at PD 0. While possible, this seems very unlikely given the data for PNS neurons. Thus, our expectation is that if developmental death of BFCN is regulated by the target, NGF was delivered during a substantial portion of this period.

A conclusion that can be drawn from this study is that, if septal BFCNs undergo developmental death postnatally, NGF produced in limited amounts in the target of these cells plays no role in regulating their survival. Although there is abundant evidence that PNS and CNS neurons respond to NGF with enhanced differentiation (Longo, et al., 1993), a role for NGF in the survival of BFCN has not been established in this or other studies. Thus, whereas limited availability of target-derived NGF regulates survival of PNS neurons, hippocampal NGF does not appear to affect the survival of septal BFCNs. We found no increase in BFCN cell number with NGF administration. Although quantitative data were not given in the NGF and trk A gene disruption studies, these experiments also failed to document an obvious decrease in the number of BFCNs (Crowley, et al., 1994, Smeyne, et al., 1994). Significantly, in these experiments, BFCN would never have had access to NGF. However, three caveats apply to the interpretation of these results. In the case of the gene disruption experiments, most animals died in

the first 3 postnatal days and few survived to 30 days. Thus, only very young animals were available for study. If substantial cell death occurs later than PD 14, little or no difference in BFCN number would have been seen. This concern does not apply to the implant experiments reported herein. A second caveat is that the NGF normally present in the hippocampus may be sufficient to ensure survival of all BFCNs. This suggestion envisions a situation in which NGF would regulate BFCN survival only when normal levels were decreased by some pathological process. One is reminded of in vitro studies in which BFCNs have clearly been shown to depend on NGF for survival (Grothe, et al., 1989, Kew, et al., 1995, Svendsen, et al., 1994). Also relevent are the in vivo studies in which target ablation resulted in loss of developing BFCNs (Burke, et al., 1995). While it is interesting that NGF can rescue BFCNs under certain experimental conditions, these data would not appear to explain the regulation of programmed cell death for this population. A final caveat is that in our control implants, there was a small increase in endogenous NGF levels at PD 12 and beyond. However, the size of this increase and its delay relative to the expected time for BFCN death argue that it did not influence BFCN survival or the interpretation of our experiments. Thus, our results and those from other laboratories employing different methods combine to suggest strongly that NGF does not regulate survival of BFCNs.

Failure to see an NGF effect on BFCN survival does not mean that target-derived neurotrophic factors have no role in this process. Indeed, several factors that act on BFCNs are produced in hippocampus. These include BDNF, NT-3, CNTF and FGF. There are data suggesting that neither BDNF nor NT-3 are important. Disruption of the genes for these neurotrophins have demonstrated no apparent decrease in BFCNs. However, as suggested above, the brief time for survival of these animals postnatally limits the interpretation. However, the CNTF knockout mouse is long-lived. Interestingly, these animals develop a progressive degenerative motor neuropathy (Masu, et al., 1993). Data characterizing the CNS of these animals are scanty, and no

documented data show a decrease in BFCNs. Basic FGF promotes differentiation and survival of BFCNs in culture (Grothe, et al., 1989) and influences the differentiation of BFCNs in vivo (Anderson, et al., 1988, Otto, et al., 1989). We know of no report for the consequences of disrupting the bFGF gene or that for its receptor on the CNS. Further studies will be required to determine whether neurotrophic factors regulate survival of BFCNs.

4.2 Slow-releasing polymer implants as an intracranial drug delivery system

In this study, a system has been devised for chronically administering NGF to neonatal rats. NGF-containing polymer implants released NGF that was fully bioactive. By placing slow-releasing NGF implants in the hippocampus, it was possible to achieve NGF levels that averaged 20 times normal over the first 2 weeks and 13 times normal over the first month. NGF released to the hippocampus resulted in a concomittant increase in NGF levels in the ipsilateral septum. NGF levels in the latter were 19 times normal during the first 2 weeks and averaged 10 times normal over the first month. The increase in ipsilateral septum suggests increased retrograde transport of exogenous NGF from the hippocampus to the septum. However, a local increase in the CSF bathing the septum is also possible. Importantly, NGF receptors are expressed on the neuronal soma as well as the neurites. Thus, NGF arriving via the CSF could be concentrated by this mechanism.

The implants were well tolerated by the animals. As expected, the surgical implant procedure caused some injury to the overlying cortex and resulted in a slight distortion of the hippocampal tissues. However, terminal staining intensity and distribution of AChE-positive fibers were comparable to the untreated hippocampus. As mentioned above, RSA-treated hippocampus also showed an increase in endogenous

NGF. This increase was reflected in a concomittant septal increase. Whether the increase in endogenous NGF level resulted from the injury inflicted during the implant placement procedure or whether this increase was brought about by RSA has not been ascertained in this study. However, the latter is more likely given the delay in the increase (not seen at PD 7 but seen at PD 12). This issue can be clarified by adding a group of animals treated with blank implants. It is worth noting that the increase in endogenous NGF levels brought about by RSA implant was not enough to compensate for the cell loss brought about by the surgical procedure (Figure 3.3 UNT/VEH vs RSA/VEH).

The main objective of the implant delivery system was to flood the hippocampus with supraphysiologic levels of NGF. Although a high level of NGF was recorded throughout the duration of the experiment, the extent of NGF diffusion into the target tissue was not evaluated directly. Thus whether there was uniform distribution of NGF throughout the hippocampus cannot be stated at present. Nevertheless, NGF is known to diffuse widely after ventricular injection. Also, studies of slow-release delivery systems have shown that molecules can diffuse up to 2-3 mm from the implant (Krewson, et al., 1995). By serial sectioning through the septum, fimbria-fornix and the the hippocampus, we found that the septum occupied 1.6 mm of the total sagittal length of the forebrain, the fimbria-fornix occupied 0.5 mm, and the hippocampus occupied 3.2 mm. Because the location of the implant was just before the mid-point of the hippocampus, it is reasonable to assume that NGF delivered from the implant diffused to the entire hippocampus.

In summary, the EVAc polymer implants can be used for long-term delivery of NGF into brain tissues. These implants slowly release bioactive NGF and can be placed to deliver NGF into a defined area.

REFERENCES

Allsopp, T. E., Wyatt, S., Paterson, H. F. and Davies, A. M. (1993). The proto-oncogene *bcl-2* can selectively rescue neurotrophic factor-dependent neurons from apoptosis. *Cell* 73, 295-307.

Altar, C. A. and Bakhit, C. (1991). Receptor-mediated transport of human recombinant nerve growth factor from olfactory bulb to forebrain cholinergic nuclei. *Brain Res* 541, 82-88.

Anderson, K. J., Dam, D. and Lee, S. C., C.W. (1988). Basic fibroblast growth factor prevents death of lesioned cholinergic neurons in vivo. *Nature* 332, 360-361.

Auburger, G., Heumann, R., Hellweg, R., Korsching, S. and Thoenen, H. (1987). Developmental changes of nerve growth factor and its mRNA in the rat hippocampus: comparison with choline acetyltransferase. *Dev. Biol.* 120, 322-328.

Barde, Y.-A. (1989). Trophic factors and neuronal survival. *Neuron* 2, 1525-1534.

Bawa, R., Siegel, R. A., Marasca, B., Karel, M. and Langer, R. (1985). An explanation for the sustained release of macromolecules from biocompatible polymers. *J. Controlled Release* 1, 259-267.

Burke, M. A., Mobley, W. C., Cho, J., Weigand, S. J., Lindsay, R. M., Mufson, E. J. and Kordowers, J. H. (1995). Loss of developing cholinergic basal forebrain neurons following excitotoxic lesions of the hippocampus: rescue by neurotrophins. *Exp. Neurol.* 130, 178-195.

Butcher, L. L. and Woolf, N. J. (1983). *Cholinergic systems in the central nervous system: retrospection, anatomic distribution and functions.* In Handbook of chemical neuroanatomy, A. a. H. Björklund T., ed. (Amsterdam: Elsevier), pp. 1-9.

Catsicas, M., Pequignot, Y. and Clarke, P. G. H. (1992). Rapid onset of neuronal death induced by blockade of either axoplasmic transpot or action potentials in afferent fibers during brain development. *J. Neurosci* 12, 4642-4650.

Cavalieri, B. (1966). *Geometria degli indivisibili.* In ed. (Torino: Unione Tipografico).

Cavicchioli, L., Flanigan, T. P., Vantini, G., Fusco, M., Polato, P., Toffano, G., Walsh, F. S. and Leon, A. (1989). NGF amplifies expression of NGF receptor messenger RNA in forebrain cholinergic neurons of rats. *Eur. J. Neurosci.* 1, 258-262.

Chao, M. V. (1992). Neurotrophin receptors: a window into neuronal differentiation. *Neuron* 9, 583-593.

Coughlin, M. D. and Collins, M. B. (1985). Nerve growth factor-independent development of embryonic mouse sympathetic neurons in dissociated cell culture. *Dev. Biol.* 110, 392-401.

Cowan, W. M. and W., F. J. (1984). Regressive events in neurogenesis. *Science* 225, 1258-1265.

Crowley, C., Spencer, S. D., Nishimura, M. C., Chen, K. S., Pitts, M. S., Armanini, M. P., Ling, L. H., MacMahon, S. B., Shelton, D. L., Levinson, A. D. and et, a. l. (1994). Mice lacking nerve growth factor display perinatal loss of sensory and sympathetic neurons yet develop basal forebrain cholinergic neurons. *Cell* 76, 1001-1011.

Cunningham, T. J., Mohler, I. M. and Giordano, D. L. (1982). Naturally occurring neuron death in the ganglion cell layer of the neonatal rat: morphology and evidence for regional correspondence with neuron death in superior colliculus. *Dev Brain Res* 2, 203.

Davies, A. and Lumsden, A. (1984). Relation of target encounter and neuronal death to nerve growth factor responsiveness in the developing mouse trigeminal ganglion. *J. Comp. Neurol.* 223, 124-137.

Davies, A. M., Bandtlow, C., Heumann, R., Korsching, S., Rohrer, H. and Thoenen, H. (1987). Timing and site of nerve growth factor synthesis in developing skin in relation to innervation and expression of the receptor. *Nature* 326, 353-358.

Eichler, M. E. and Rich, K. M. (1989). Death of sensory ganglion neurons after acute withdrawal of nerve growth factor in dissociated cell cultures. *Brain Research* 482, 340-346.

Estus, S., Zaks, W. J., Gruda, M., Bravo, R. and Johnson, E. M. J. (1994). Altered gene expression during programmed cell death: identification of c-jun as necessary for neuronal apoptosis. *J. cell Biol.* 127, 1717-1727.

Fischer, W., Chen, K. S., Gage, F. H. and Björklund (1991). Progressive decline in spatial learning and integrity of forebrain cholinergic neurons in rats during aging. *Neurobiol. of Aging* 13, 9-23.

Fishman, R. A. (1992). *Cerebrospinal fluid in diseases of the nervous system.* In ed. (Philadelphia: W.B. Saunders Co., Harcourt Bruce Jovanovich, Inc.), pp. 204

Franklin, J. L., Sanz-Rodriguez, L., Juhasz, A., Deckwerth, T. L. and Johnson, E. M. J. (1995). Chronic depolarization prevents programmed death of sympathetic neurons in vitro but does not support growth: requirement for Ca2+ influx but not Trk activation. *J. Neurosci.* 15, 143-164.

Garcia, I., Martinou, I., Tsujimoto, Y. and Martinou, J.-C. (1992). Prevention of programmed cell death of sympathetic neurons by the *bcl*-2 proto-oncogene. *Science* 258, 302-304.

Glucksmann (1951). Cell deaths in normal vertebrae ontogeny. *Biol Rev* 26, 59.

Gnahn, H., Hefti, F., Heumann, R., Schwab, M. E. and Thoenen, H. (1983). NGF-mediated increase of choline acetyltransferase (ChAT) in the neonatal rat forebrain : evidence for a physiological role of NGF in the brain. *Dev. Brain Res.* 9, 42-52.

Grimes, M., Zhou, J., Li, Y., Holtzman, D. and Mobly, W. C. (1993). Neurotrophin signalling in the nervous system. *Sem. Neurosci.* 5, 239-247.

Grothe, C., Otto, D. and Unsicker, K. (1989). Basic fibroblast growth factor promotes in vitro survival and cholinergic development of rat septal neurons: comparison with the effects of nerve growth factor. *Neurosci.* 3, 649-661.

Gunderson, H. J. G. (1986). Stereology of of arbitrary particles. *J. Microsci* 143, 3-45.

Gunderson, H. J. G. and Jensen, E. B. (1987). The efficiency of systematic sampling in stereology and its prediction. *J. Microsci.* 147, 229-263.

Hamburger, V., Brunso-Bechtold, J. K. and Yip, J. W. (1981). Neuronal death in the spinal ganglia of the chick embryo and its reduction by NGF. *J. Neurosci.* 1, 60-71.

Hedreen, J. C., Portera-Cailliau, C., Price, D. L. and Koliatsos, V. E. (1994). Patterns of tunel labeling and non-random DNA fragmentation in Huntington disease. *Soc Neurosci. Abs.* 20, 250.

Hefti, F. (1986). Nerve growth factor (NGF) promotes survival of septal cholinergic neurons after fimbrial transection. *J. Neurosci.* 6, 2155-2162.

Henderson, C. E., Camu, W., Mettling, C., Gouin, A., Poulsen, K., Karihaloo, M., Rullamas, J., Evans, T., McMahon, S. B., Armanini, M. P., Berkemeier, L., Phillips, H. S. and Rosenthal, A. (1993). Neurotrophins promote motor neuron survival and are present in embryonic limb bud. *Nature* 363, 266-270.

Hendry, I. A. (1975). The response of adrenergic neirones to axotomy and nerve growth factor. *Brain Res.* 94, 87-97.

Hendry, I. A. and Campbell, J. (1976). Morphometric analysis of rat superior cervical ganglion after axotomy and nerve growth factor treatment. *J. Neurocytol.* 5, 351-360.

Hendry, I. A. and Iversen, L. L. (1973). Changes in tissue and plasma concentrations of NGF following the removal of the submaxillary glands in adult mice and their effects on the sympathetic nervous system. *Nature* 243, 500-504.

Hengartner, M. O., Ellis, R. E. and Horvitz, H. R. (1992). *Caenorhabditis elegans* gene *ced-9* protects cells from programmed cell death. *Nature* 356, 494-499.

Heumann, R., Korsching, S., Brandtlow, C. and Thoenen, H. (1987). Changes in NGF systhesis in non-neuronal cells in response to sciatic nerve transection. *J. Cell Biol.* 104, 1623-1631.

Heumann, R., Korsching, S., Scott, J. and Thoenen, H. (1984b). Relationship between levels of nerve growth factor (NGF) and its messenger RNA in sympathetic ganglia and peripheral target tissues. *Embo J* 3, 3183-3189.

Heumann, R., Schwab, M., Merkl, R. and Thoenen, H. (1984a). Nerve growth factor-mediated induction of choline acetyltransferase in PC12 cells: evaluation of the site of action of nerve growth factor and the involvement of lysosomal degradation products of nerve growth factor. *J Neurosci* 4, 3039-3050.

Higgins, G. A., Koh, S., Chen, K. S. and Gage, F. H. (1989). NGF induction of NGF receptor gene expression and cholinergic neuronal hypertrophy within the basal forebrain of the adult rat. *Neuron* 3, 247-256.

Hoffman, D., Wahlberg, L. and Aebischer, P. (1990). NGF released from a polymer matrix prevents loss of ChAt expression in the basal forebrain neurons following a fimbria-fornix lesion. *Exp Neurology* 110, 39-44.

Holtzman, D. M., Kilbridge, J., Bredt, D. S., Black, S. M., Li, Y., Clary, D. O., Reichardt, L. F. and Mobley, W. C. (1995). NOS induction by NGF in basal forebrain cholinergic neurones: evidence for regulation of brain NOS by a neurotrophin. *Neurobiol. Disease* 1, 51-60.

Holtzman, D. M., Kilbridge, J., Li, Y., Cunningham, E. T., Lenn, N. J., Clary, D. O., Reichardt, L. F. and Mobley, W. C. (1994). TrkA expression in the CNS: Evidence for the existence of several novel NGF-responsive CNS neurons. *J. Neurosci.* 15,1567-1576.

Holtzman, D. M., Li, Y., Parada, L. F., Kinsman, S., Chen, C. K., Valletta, J. S., Zhou, J., Long, J. and Mobley, W. C. (1992). p140trk mRNA marks NGF-responsive forebrain neurons: evidence that *trk* gene expression is induced by NGF. *Neuron* 9, 465-478.

Johnson, E. M. and Gorin, P. G. (1980). Dorsal Root Ganglion Neurons Are Destroyed by Exposure in utero to Maternal Antibody to Nerve Growth Factor. *Science* 210, 916-918.

Johnston, M. V., Rutkowski, J. L., Wainer, B. H., Long, J. B. and Mobley, W. C. (1987). NGF effects on developing forebrain cholinergic neurons are regionally specific. *Neurochem. Res.* 12, 985-994.

Kennedy, T. E., Serafini, T., de la Torre, J. R. and Tessier-Lavigne, M. (1994). Netrins are diffusible chemotropic factors for commissural axons in the enbryonic spinal chord. *Cell* 78, 425-435.

Kennedy, T. E. and Tessier-Lavigne, M. (1995). Guidance and induction of branch formation in developing axons by target-derived diffusible factors. *Current Biol.* 5, 83-90.

Kew, J. N. C., Smith, D. W. and Sofroniew, M. V. (1995). NGF withdrawal induces apoptotic death of developing septal cholinergic neurons in vitro: pretection by cAMP and high k^+. *in press*

Koh, S., Chang, P., Collier, T. J. and Loy, R. (1989b). Loss of NGF receptor immunoreactivity in basal forebrain neurons in age rats: correlation with spatial memory impairment. *Brain Res* 498, 397-404.

Koh, S. and Loy, R. (1989a). Localization and Development of Nerve Growth Factor-Sensitive Rat Basal Forebrain Neurons and their Afferent Projections to Hippocampus and Neocortex. *J Neuroscience* 9, 2999-3018.

Koliatsos, V. E., Applegate, M. D., Knusel, B., Junard, E. O., Burton, L. E., Mobley, W. C., Hefti, F. F. and Price, D. L. (1991). Recombinant human nerve growth factor prevents retrograde degeneration of axotomized basal forebrain cholinergic neurons in the rat. *Exp Neurol* 112, 161-73.

Korsching, S., Auburger, G., Heumann, R., Scott, J. and Thoenen, H. (1985). Levels of nerve growth factor and its mRNA in the central nervous system of the rat correlate with cholinergic innervation. *Embo J* 4, 1389-13
93.

Korsching, S. and Thoenen, H. (1983). Nerve growth factor in sympathetic ganglia and corresponding target organs of the rat: correlation with density of sympathetic innervation. *Proc Natl Acad Sci U S A* 80, 3513-3516.

Korsching, S. and Thoenen, H. (1985). Nerve growth factor supply for sensory neurons: site of origin and competition with the sympathetic nervous system. *Neurosci Lett* 54, 201-205.

Krewson, C. E., Klarman, M. L. and Saltzman, W. M. (1995). Distribution of nerve growth factor following direct delivery to brain interstitium. *Brain Res.* in press,

Kromer, L. F. (1987). Nerve growth factor treatment after brain injury prevents neuronal death. *Science* 235, 216-218.

Large, T. H., Bodary, S. C., Clegg, D. O., Weskamp, G., Otten, U. and Reichardt, L. F. (1986). Nerve growth factor gene expression in the developing rat brain. *Science* 234, 352-355.

Levi-Montalcini, R. (1987). The Nerve Growth Factor 35 Years Later. *Science* 237, 1154-1161.

Levi-Montalcini, R. and Angeletti, P. U. (1968). Nerve growth factor. *Physiol. Rev.* 48, 534-569.

Levi-Montalcini, R. and Booker, B. (1960). Destruction of the Sypathetic Ganglia in Mammals by and Antiserum to a Nerve Growth Protein. *Proc. Natl. Acad. Sci. USA* 46, 384-391.

Levi-Montalcini, R. and Cohen, S. (1956). In vitro and in vivo effects of a nerve growth-stimulating agent isolated from snake venom. *PNAS, USA* 42, 695.

Levi-Montalcini, R. and Hamburger, V. (1951). Selective growth stimulating effects of mouse sarcoma on the sensory and sympathetic nervous system of the chick embryo. *J. Exp. Zool.* 116, 321-362.

Li, Y., Holtzman, D. M., Kromer, L. F., Kaplan, D. R., Chua-Couzens, J., Clary, D. O., Knusel, B. and Mobley, W. C. (1995). Coordinate regulation of *TrkA* and *ChAT* expression in developing rat basal forebrain: evidence that endogenous NGF regulates differentiation of cholinergic neurons. *J. Neurosci.* (in press),

Loeb, D. M., Maragos, J., Martin-Zanca, D., Chao, M. V., Parada, L. F. and Greene, L. A. (1991). The trk proto-oncogene rescues NGF responsiveness in mutant NGF-nonresponsive PC12 cell lines. *Cell* 66, 961-966.

Longo, F. M., Holtzman, D. M., Grimes, M. L. and Mobley, W. C. (1993). Nerve Growth Factor: Actions in the Peripheral and Central Nervous Systems. In *Neurotrophic Factors*,J. Fallon and S. Loughlin, ed. (New York: Academic Press), pp. 209-256.

Markowski, A. L., Koliatsos, V. E., Breckler, S. J., Price, D. L. and Olton, D. S. (1994). Human nerve growth factor improves spatial memory in aged but not young rats. *J. Neurosci* 14, 4815-4824.

Martin, D. P. and Johnson, E. M. (1991). Programmed cell death in the peripheral nervous system. In *Apoptosis: The Molecular Biology of Cell Death*,L. D. Tomei and F. O. Cope, ed. (Cold Spring Harbor, N Y: Cold Spring Harbor Laboratory Press), pp. 247-262.

Martin, D. P., Schmidt, R. E., DiStefano, P. S., Lowry, O. H., Carter, J. G. and Johnson Jr., E. M. (1988). Inhibitors of Protein Synthesis and RNA synthesis Prevent Neuronal Death Caused by Nerve Growth Factor Deprivation. *J. Cell Biol.* 106, 829-844.

Masu, Y., Wolf, E., Holtmann, B., Sendtner, M., Brem, G. and Thoenen, H. (1993). Disruption of CNTF gene results in motor neuron degeneration. *Nature* 365, 27-30.

McGeer, P. L., McGeer, E. G., Kimura, H. and Peng, J. F. (1983). *Cholinergic neurons and cholinergic projections in the mammalian CNS.* In Handbook in chemical neuroanatomy, A. a. H. Björklund T, ed. (Amsterdsm: Elsevier), pp. 11-21.

Meakin, S. O., Suter, U., Drinkwater, C. C., Welcher, A. A. and Shooter, E. M. (1992a). The rat trk protooncogene product exhibits properties characteristic of the slow nerve growth factor receptor. *Proc. Natl. Acad. Sci. USA* 89, 2374-2378.

Milner, T. A., Loy, R. and Amaral, D. G. (1983). An anatomical study of the development of the septo-hippocampal projection in the rat. *Dev. Brain Res.* 8, 343-371.

Mobley, W. C., Neve, R. L., Prusiner, S. B. and McKinley, M. P. (1988). Nerve growth factor increases mRNA levels for the prion protein and the beta-amyloid protein precursor in developing hamster brain. *Proc. Natl. Acad. Sci. U S A* 85, 9811-9815.

Mobley, W. C., Rutkowski, J. L., Tennekoon, G. I., Gemski, J., Buchanan, K. and Johnston, M. V. (1986). Nerve growth factor increases choline acetyltransferase activity in developing basal forebrain neurons. *Mol. Brain Res.* 387, 53-62.

Mobley, W. C., Rutkowski, J. L., Tennekoon, S. J., Buchanan, K. and Johnston, M. V. (1985). Choline acetyltransferase in striatum of neonatal rats increased by nerve growth factor. *Science* 229, 284-287.

Mobley, W. C., Woo, J. E., Edwards, R. H., Riopelle, R. J., Longo, F. M., Weskamp, G., Otten, U., Valletta, J. S. and Johnston, M. V. (1989). Developmental regulation of nerve growth factor and its receptor in the rat caudate-putamen. *Neuron* 3, 655-664.

Mouton, P., Pakkenberg, B., Gunderson, H. J. and Price, D. L. (1994). Absolute number abd size of pigmented locus coeruleus neurons in young and aged individuals. *J. Chem. Neuroanatomy* 7, 185-190.

Murray, J. B., Brown, L., Langer, R. and Klagsburn, M. (1983). A micro sustained release system for epidermal growth factor. *In Vitro* 19, 743-748.

Oppenheim, R. W. (1989). The neurotrophic theory and naturally occurring motoneuron death. *Trends Neurosci* 12, 252-255.

Oppenheim, R. W., Prevette, D., Qin-Wei, Y., Collins, F., MacDonald, J. (1991). Control of embryonic motoneuron survival in vivo by ciliary neurotrophic factor. *Science* 251, 1616-1618.

Oppenheim, R. W., Prevette, D., Tyntell, M. and Homma, S. (1990). Naturally ocurring and induced neuronal death in the chick embryo in vivo requires protein and RNA synthesis: evidence for the role of cell death genes. *Devel. Biol.* 138, 104-113.

Otto, D., Frotscher, M. and Unsicker, K. (1989). Basic fibroblast growth factor and nerve growth factor administered in gel foam rescue medial septal neurons after fimbria fornix transection. *J. Neurosci. Res.* 22, 83-91.

Rhine, W. D., Hsieh, D. S. T. and Langer, R. (1980). Polymers for sustained macromolecule release: Procedures to fabricate reproducible delivery systems and control release kinetics. *J. Pharm. Sci.* 69, 265-270.

Richardson, P. M. and Riopelle, R. J. (1984). Uptake of nerve growth factor along peripheral and spinal axons of primary sensory neurons. *J Neurosci* 4, 1683-1689.

Saunders, J. W. (1966). Death in embryonic systems. Death of cell sis the usual accompaniment of embryonic growth and differentiation. *Science* 154, 604.

Schechter, A. L. and Bothwell, M. A. (1981). Nerve growth factor receptors on PC12 cells: evidence for two receptor classes with differing cytoskeletal association. *Cell* 24, 867-874.

Schwab, M. E., Otten, U., Agid, Y. and Thoenen, H. (1979). Nerve growth factor (NGF) in the rat CNS: absence of specific retrograde axonal transport and tyrosine hydroxylase induction in locus coeruleus and substantia nigra. *Brain Res* 168, 473-483.

Scott, S. A. and Davies, A. M. (1990). Inhibition of protein synthesis prevents cell death in sensory and parasympathetic neurons deprived of neurotrophic factor in vitro. *J. Neurobiol.* 21, 630-638.

Seiler, M. and Schwab, M. E. (1984). Specific retrograde transport of nerve growth factor (NGF) from neocortex to nucleus basalis in the rat. *Brain Res* 300, 33-39.

Serafini, T., Kennedy, T. E., Galko, M. J., Mirzayan, C., Jessell, T. M. and Tessier-Lavigne, M. (1994). The netrins define a family of axon outgrowth-promoting proteins homologous to C.elegans UNC-6. *Cell* 78, 409-424.

Server, A. C. and Mobley, W. C. (1991). Neuron Cell Death and the Role of Apoptosis. In *Apoptosis: The Molecular Biology of Cell Death*,L. D. Tomei and F. O. Cope, ed. (Cold Spring Harbor, N Y: Cold Spring Harbor Laboratory Press), pp. 263-278.

Shelton, D. L. and Reichardt, L. F. (1986). Studies on the expression of beta NGF gene in the central nervous system: Level and regional distribution of NGF mRNA suggest

that NGF functions as a trophic factor for several neuronal populations. *Proc. Natl. Acad. Sci. USA* 83, 2714-2718.

Siegel, R. A. and Langer, R. (1984). Controlled release of polypeptides and other macromolecules. *Pharm Res* 1, 1-10.

Siegel, R. A. and Langer, R. (1990). Mechanistic studies of macromolecular drug release from macropopous polymers. II. Models for the slow kinetics of drug release. *J. Controlled Release* 14, 153-167.

Smeyne, R. J., Klein, R., Schnapp, A., Long, L. K., Bryant, S., Lewin, A., Lira, S. A. and Barbacid, M. (1994). Severe sensory and sympathetic neuropathies in mice carrying a disrupted Trk/NGF receptor gene. *Nature* 368, 246-249.

Sofroniew, M. V., Cooper, J. D., Svendsen, C. N., Crossman, P., Ip, N. Y., Lindsay, R. M. and Zafra, F. (1993). Atrophy but not death of adult septal cholinergic neurons after ablation of target capacity to produce mRNA for NGF, BDNF, and NT3. *J. Neurosci.* 13, 5263-5276.

Sofroniew, M. V., Galletly, N. P., Isacson, O. and Svendsen, C. N. (1990). Survival of adult basal forebrain cholinergic neurons after loss of target neurons. *Science* 247, 338-342.

Svendsen, C. N., Kew, J. N. C., Staley, K. and Sofroniew, M. V. (1994). Death of developing septal cholinergic neurons following NGF withdrawal in vitro: Protection by protein synthesis inhibition. *J. Neurosci.* 14, 75-87.

Thoenen, H. and Barde, Y.-A. (1980). Physiology of Nerve Growth Factor. *Physiol. Rev.* 60, 1284-1335.

Weskamp, G. and Otten, U. (1987). An enzyme-linked immunoassay for nerve growth factor: A tool for studying regulatory mechanisms involved in NGF production in brain and peripheral tissues. *J. Neurochem.* 48, 1779-1786.

West, M. J. (1993). New sterological methods for counting neurons. *Neurobiology of Aging* 14, 275-285.

West, M. J., Slomianka, L. and Gunderson, H. J. G. (1991). Unbiased stereological estimation of the total number of neurons in the subdivisions os the rat hippocampus using the optical fractionator. *Anat. Rec.* 231, 482-497.

Wilcox, B. J. and Kitt, C. A. (1994). Evidence for substantia nigra neuronal cell death in Rett syndrome using TUNEL histochemistry. *Soc. Neurosci. Abs.* 20, 688.

Williams, G. T. and Smith, C. A. (1993). Molecular regulation of apoptosis: Genetic controls on cell death. *Cell* 74, 777-779.

Williams, L. R., Varon, S., Peterson, G. M., Wictorin, K., Fischer, W., Bjorklund, A. and Gage, F. H. (1986). Continuous infusion of nerve growth factor prevents basal forebrain neuronal death after fimbria-fornix transection. *Proc. Natl. Acad. Sci. USA* 83, 9231-9235.

Williams, R. W. and Herrup, K. (1988). The control of neuron number. *Annu Rev Neurosci* 11, 423-53.

Wright, L. L., Cunningham, T. J. and Smolen, A. J. (1983). Developmental neuron death in the rat superior cervical sympathetic ganglion: cell counts and ultrastructure. *J. Neurocytol.* 12, 727-738.

Yan, Q., Matheson, C., Sun, J., Radeke, M. J., Feinstein, S. C. and Miller, J. A. (1994). Distribution of intracerebral ventricularly administered neurotrophins in rat brain and its correlation with trk receptor expression. *Exp. Neurol.* 127, 23-36.

Appendix A:

Table of recipes in the preparation of polymer blocks

Polymer Block	Loading Volume	EVAc/mg	Dichloro-methane/ml	NGF-RSA/mg
NGF_{90}	30%	200	2	60
NGF_{180}	40%	200	2	80
NGF_{250}	40%	200	2	80

Appendix B:

Enzyme-Linked Immunoadsorption Assay (ELISA)

(modified from Weskamp and Otten 1987)

NGF standards and liquid sample preparation for ELISA:

NGF stock solution was serially diluted to the desired concentration (15 pg/ml–8 ng/ml) using a sample buffer of 0.5% BSA, 20 kI/ml aprotinin, 0.1 mM phenymethyl sulfonyl flouride (PMSF), and 0.1 mM benzethonium chloride in 10 mM PBS. Liquid samples (obtained from experiments on the in vitro release of NGF from polymer implants) were prepared using the same sample buffer at 1:50–1:2000 dilution, NGF standards and liquid samples at 100 µl/well were then used to assay for NGF levels.

Dissection Procedure for Medial Septum and Hippocampus:

Rat pups were euthanized by an overdose of sodium pentobarbital delivered intraperitoneally. Each brain was collected immediately and transferred onto an ice stage. The brain was cut sagittally into its right and left halves. Each half was flipped to expose the cut medial surface. The medial septum is clearly visible just underneath the frontal cortex as it starts ventrally and extends up in a dorso-caudal direction to form the fimbria fornix. Using a pair of curved microsurgical forceps, the septum was nipped

free at its fornix junction and scooped out using the same instrument. The collected septum was then quick-frozen on a slab of dry ice. The hippocampus was collected by first dissecting out the thalamus and caudate putamen using the same forceps, then carefully nipping off the cerebellum and brain stem, leaving the entire cortex and hippocampus intact. At this point, the hippocampus can be seen curling around the lateral cortex in a dorso-ventral direction. The hippocampus was carefully dissected free of its connections along the cortex on both the dorso-medial and ventro-lateral surfaces. The forceps was then inserted between the junction of the hippocampus and lateral cortex. The hippocampal structure was then gently lifted out by sliding the forceps along the length of the hippocampus. The speciman was quick-frozen as above. Finally, the frozen septa and hippocampi were transferred into labeled eppendorf tubes and stored frozen at -70^{o}C until assayed.

Brain tissue sample preparation for ELISA:

Septal and hippocampal tissue samples were mixed with sample buffer (same sample buffer as in liquid sample preparation above) at a 1:9,1:19, or 1:29 (mg tissue:µl sample buffer) dilution, sonicated (Sonicator™ Cell Disruptor,Ultrasonics, Plainview, NY) for 30 seconds at 4^{o}C and centrifuged at 3000xg for 20 minutes in the cold room. The supernatants were then collected and 100µl/well were used to assay for NGF levels.

Assay Method:

NUNC™ Immunosorb plates were coated with 100 µl/well of polyclonal goat anti-mouse NGF (GAM) antibody and pre-immune goat serum (GIG) on alternate rows (refer to diagram of plate setup below). Antibody and control solutions were prepared by diluting GAM and GIG (1:1000) in coating buffer (a solution of 3 mM sodium azide, 50 mM sodium carbonate and 50 mM sodum bicarbonate). The plates were allowed to coat overnight at 4^{o}C on a shaker, washed for 3x5 minutes with washing buffer (0.05%

Tween-20 in 10 mM PBS), air dried, and blocked with 200 µl/well of 5% fetal calf serum (FCS) in 10 mM PBS for 2 hours at room temperature on a shaker. The blocking solution was then washed away 3x5 minutes with washing buffer and air dried. Serially diluted NGF standards (15 pg/ml–8 ng/ml) at 100 µl/well were plated into the top and bottom 2 rows of the plate (refer to diagram of plate setup below). Diluted samples (see above for sample preparations) at 100 µl/well were then plated into the middle 4 rows of the plate (refer to diagram of plate setup below). Reaction procedure was carried out by incubating the plates overnight at 4°C on a shaker. After the plates were washed and dried as above, 100 µl/well of monoclonal anti-rat NGF (1G3) at 1:200 dilution in 1% FCS/10 mM PBS with 0.1% Tween-20 (PBST) solution was plated on all 96 wells. Incubation was carried out on a shaker overnight at 4°C. After washing and drying, 100 µl/well of biotinylated goat anti-rat antibody at 1:5000 dilution in 1% FCS-PBST solution was plated and incubated overnight at 4°C on a shaker. The plates waere washed and dried as above and 100 µl/well of strepavidin horseradish peroxidase (SA-HRP) at 1:2000 dilution in 1% FCS-PBS was plated and incubated for 2 hours at room temperature on a shaker. Color development was carried out after washing and drying by adding 100 µl of substrate solution (4 mM orthophenylendiamine (Sigma) in phosphate citrate buffer plus 0.02% hydrogen peroxide) for 5–10 minutes. The reaction was stopped by adding 50 µl/well of 2.5 M sulfuric acid. Color development was then measured by its absorbance at a wavelength of 492nm in a Titertek™ plate reader.

Final color reading was obtained by subtracting the GIG (background) reading from the GAM reading. A standard curve was then generated by non-linear least square fitting of all the data points. NGF levels from the samples were then estimated from the standard curve.

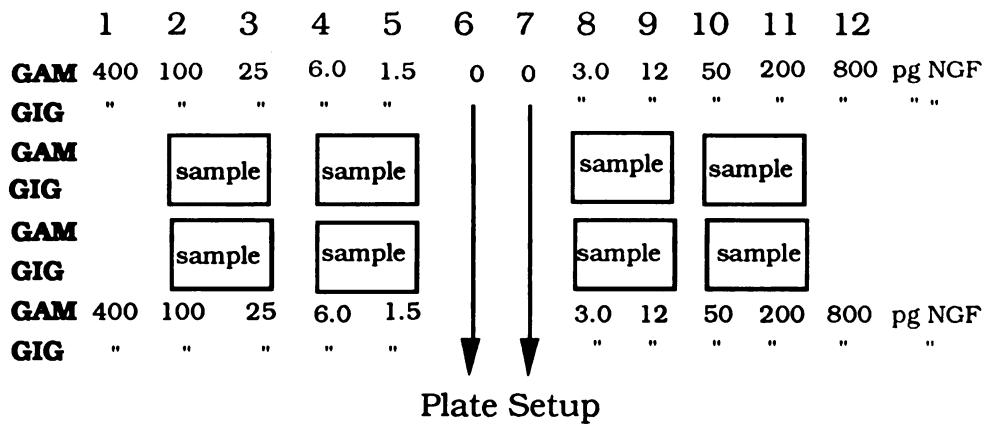

Figure 2. ELISA plate setup showing the top and bottom GAM/GIG rows plated with serially diluted NGF standards to generate a standard curve. The boxed wells in the middle section of the plate were plated with liquid (from in vitro NGF release experiments) or tissue (from in vivo NGF release experiments) samples.

Appendix C:

Chick Dorsal Root Ganglia (DRG) bioassay

DRG assay was carried out as described (Davies, 1989) with some modifications. A 96-well tissue culture plate (Costar 3696) was prepared by coating the wells with poly-L-ornithine in PBS solution (2 μg/ml) for 1 hour at room temperature. The wells were washed with double distilled water and the following solutions plated into each column of the plate as outlined in the diagram below) culture media (DME H16 with pen-strep) with 10% FCS alone (as control); 2) serial dilution of NGF in culture media with 10% FCS (1.5 to 200 pg NGF/ml, for generating the NGF standard curve); 3) 100 pg NGF/ml of the samples (supernatants from NGF implants), and 4) the same amount as 3) of supernatants from RSA and blank implants. The plate was set aside in the incubator until the DRG cells were ready to be plated.

Dorsal rool ganglia were dissected from 8-day-old chick embryos in PBS and collected in Hank's balanced salt solution-calcium and magnesium-free (BSS-CMF)

medium. Dissociation of the cells was achieved by trypsinization (0.08% trypsin) for 20 minutes at 37°C and gentle trituration in culture media supplemented with 10% FCS. A homogeneous neuronal population was collecte—by plating the cell suspension in Facon 3003 plates and incubating in a humidified CO_2 incubator at 37°C for 1 hour and 50 minutes for differential attachment of the non-neuronal cells of the gangli—and were then plated at 2500 cells/well into the prepared plate and incubated in a humidified CO_2 incubator at 37°C. After 24 hours, the cells were fixed in 2% gluteraldehyde solution and the number of cells that had grown neurites on cell body length were then counted in each well. A standard NGF activity curve was then generated by subtracting the background activity (average cell number in control lanes) from the lanes containing serially diluted NGF. Bioactivity of the sample was derived by comparing the corrected average cell number (sample lane - average control lane) of the sample lane (which contained 100 pg/ml of NGF) with the average cell number counted from the standard curve at 100 pg/ml NGF and expressed as percent 100 pg/ml NGF.

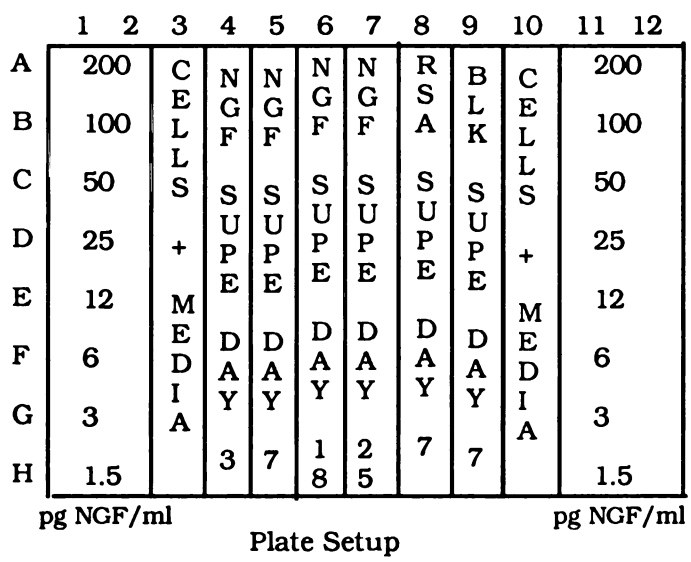

Figure 3. DRG bioassay plate setup

Columns 3 &10 were plated with media alone+ cells to serve as controls
Columns 1,2, 11 &12 were plated with serial dilutions of NGF+ media + cells to generate a standard NGF activity curve.
Columns 4-7 were plated with supernatants from the same NGF implant collected at day 3,7,18 & 25 of the NGF release experiment. Supe contained approximately 100 pg NGF/ml.
Wells in column 8 were plated with supernatants from an RSA implant collected at day 7.
Column 9 contain supernatants from a blank implant collected at day 7.


UC
San Francisco
LIBRARY

For reference

Not to be taken from the room.

6357365

3 1378 00635 7365